Sienna Technical Report No. 974

HIGH THERMAL CONDUCTIVITY AlN PACKAGES FOR HIGH-TEMPERATURE ELECTRONICS

E. Savrun and C. Toy, Sienna Technologies, Inc.

M. Sarikaya, University of Washington

September 1998

Prepared for

AIR FORCE OFFICE OF SCIENTIFIC RESEARCH
BOLLING AIR FORCE BASE
DC 20332-8050

Final Report for Period Covering
January 10, 1996 – August 31,1998
Under Contract No. F49620-96-C-0008

Approved for Public Release; STTR Report, Distribution Unlimited.

SIENNA TECHNOLOGIES, INC.
19501 144th Avenue NE, Suite F-500
Woodinville, WA 98072-8424
Phone (425) 485-7272 Fax (425) 485-8651

Sienna Technical Report No. 974

HIGH THERMAL CONDUCTIVITY AlN PACKAGES FOR HIGH-TEMPERATURE ELECTRONICS

E. Savrun and C. Toy, Sienna Technologies, Inc.

M. Sarikaya, University of Washington

September 1998

Prepared for

AIR FORCE OFFICE OF SCIENTIFIC RESEARCH
BOLLING AIR FORCE BASE
DC 20332-8050

Final Report for Period Covering
January 10, 1996 – August 31,1998
Under Contract No. F49620-96-C-0008

SIENNA TECHNOLOGIES, INC.
19501 144th Avenue NE, Suite F-500
Woodinville, WA 98072-8424
Phone (425) 485-7272 Fax (425) 485-8651

REPORT DOCUMENTATION PAGE

Form Approved
OMB No. 0704-0188

1. AGENCY USE ONLY (Leave Blank)	2. REPORT DATE	3. REPORT TYPE AND DATES COVERED
	September 1998	Final Report 10 Jan 96 - 31 Aug 98

4. TITLE AND SUBTITLE
High Thermal Conductivity AlN Packages for High Temperature Electronics

5. FUNDING NUMBERS
F49620-96-C-0008
STTR/TS
65502F

6. AUTHOR(S)
E. Savrun, C. Toy, M. Sarikaya

7. PERFORMING ORGANIZATION NAME(S) AND ADDRESS(ES)
Sienna Technologies, Inc.
19501 144th Avenue NE, Suite F-500
Woodinville, WA 98072-6426

8. PERFORMING ORGANIZATION REPORT NUMBER
Sienna Technical Report No. 974

9. SPONSORING/MONITORING AGENCY NAME(S) AND ADDRESS(ES)
Air Force Office of Scientific Research
110 Duncan Avenue NE, Suite B115
Bolling AFB, DC 20332-8050

10. SPONSORING/MONITORING AGENCY REPORT NUMBER

11. SUPPLEMENTARY NOTES

12a. DISTRIBUTION/AVAILABILITY STATEMENT
Approved for Public Release; [redacted]
Distribution Unlimited

12b. DISTRIBUTION CODE

13. ABSTRACT (Maximum 200 words)

A novel metallization for aluminum nitride substrates and related interconnection materials were investigated for packaging silicon carbide devices for use at temperatures up to 600°C. Aluminum nitride substrates were metallized with refractory metals using both thin and thick film metallization techniques. Excellent metallization adhesions (≥ 10 ksi) were achieved at low sheet resistivities for both films. Phase diagrams were used to select potential bond pad, die attach and wire bond materials. Diffusion couples were constructed to screen the selected candidates. Gold and platinum were found to be stable bond pad materials on the refractory metallizations at 700°C. Gold-gold and platinum-platinum pad-wire combinations were suitable for use at temperatures of 600°C and beyond. Platinum-gold, copper-gold, and nickel-gold pad-wire combinations could be used with refractory metallized aluminum nitride substrate up to 400°C.

14. SUBJECT TERMS
Aluminum Nitride, Ceramic Package, High-Temperature Electronics, Interconnects, Metallization, Silicon Carbide Device

15. NUMBER OF PAGES
45

16. PRICE CODE

17. SECURITY CLASSIFICTION OF REPORT	18. SECURITY CLASSIFICATION OF THIS PAGE	19. SECURITY CLASSIFICATION OF ABSTRACT	20. LIMITATION OF ABSTRACT
Unclassified	Unclassified	Unclassified	Unlimited

Standard form 298 (Rev. 2-89)
Prescribed by ANSI Std. Z39-18
298-102

REF D

TABLE OF CONTENTS

LIST OF FIGURES

LIST OF TABLES

1. INTRODUCTION

The keys to successful high-temperature electronics are the availability of stable high-temperature electronic components (integrated circuits, resistors, capacitors, etc.) and the packaging of these components using the proper materials. The development of silicon carbide integrated circuit (SiC IC) devices for use at temperatures up to 600°C has been well underway for these applications. But without parallel developments in packaging technology, the advances in SiC ICs will not much matter. Unless there is a way for the SiC ICs to communicate with the outside world, they will not be useful. Package selection and development are critical factors in meeting several key requirements: thermal and electrical performance, cost, and form factor. Even though aluminum nitride and other ceramic packages are available for room-temperature electronics, none of them is suitable to package SiC ICs for high-temperature and/or high-power applications. Off-the-shelf packages lack thermal conductivity, thermal expansion coefficient (CTE) match to the silicon carbide, and stable metallization at high temperatures. Therefore, there is a significant need for a package development for SiC ICs suitable for continuous operation at temperatures of 600°C and above.

In this Phase II STTR project, Sienna Technologies, Inc., and the University of Washington have continued the Phase I research to identify the necessary elements for an aluminum nitride packaging for SiC devices for high-temperature (600°C and above) operation. This final report documents the Phase II effort.

2. HIGH-TEMPERATURE PACKAGING DESIGN ISSUES

Packaging a semiconductor device includes the selection of a package design and package construction materials. Material properties can significantly impact how well the package can meet its requirements. The design of high-temperature packages is primarily influenced by the available materials. High-temperature packaging design issues include the following:

- ***Thermal conductivity***: The Air Force MEA program involves power devices such as motor controls that produce large amounts of heat, up to 100 W/cm^2 (Mahefkey, 1994). These devices require a high-thermal-conductivity path for removing heat to maintain the die at a safe operating temperature. If the die temperature exceeds the safe operating temperature, the device will fail prematurely. Therefore, system thermal resistance must be minimized. Substrate, metallization, and die attach thermal conductivity must be maximized. The fact that the thermal conductivity of packaging materials decreases with increasing temperature must be considered.
- ***Thermomechanical compatibility***: Thermal expansion differences between the die and the package as well as between the different packaging components result in stresses during assembly as well as during operation that can result in the failure of the package or the device. The thermal expansion mismatch between the die, the substrate, and other packaging components should be small at all temperatures to minimize thermal stresses. Thermal expansion mismatch may increase with temperature and can aggravate the thermal stress problem.
- ***Chemical compatibility:*** Metallization should not react with the die and the substrate at assembly and service temperatures. Electromigration of conductors must be prevented or minimized to prevent failures by shorting. The temperature coefficient of resistance should be as small as possible within the intended temperature range.
- ***Hermeticity:*** The package should have atmospheric integrity to protect the die from environmental elements.
- ***Simplicity, size, and weight***: The package should be readily manufacturable, small in size, and light-weight for aircraft and space applications. The package material properties dictate the form factor.

3. HIGH-TEMPERATURE PACKAGING MATERIALS

3.1 Substrates

A survey of current packaging materials, shown in Table 1, suggests that aluminum nitride is an ideal candidate for high-power, high-temperature packaging applications. Some of the important advantages of AlN include high thermal conductivity (200 $W \bullet m^{-1} \bullet K^{-1}$), which decreases only slightly with increasing temperature (Figure 1); a coefficient of thermal expansion (4.1 x 10^{-6} $°C^{-1}$) that closely matches those of Si (3.5 x 10^{-6} $°C^{-1}$), and SiC (3.7 x 10^{-6} $°C^{-1}$) (Figure 2), which minimizes thermal stresses; good thermal shock resistance and environment stability at high temperatures; nontoxicity (unlike beryllia); high electrical resistivity; high mechanical strength; and chemical inertness at high temperatures. Dielectric constant (Table 2) and dielectric loss (Table 3) of AlN changes little with temperature up to 800°C.

Before the potential of AlN for high-temperature, high-power electronic packaging is realized, however, the related metallization issues have to be resolved. In this phase of research, we have continued addressing metallization issues for aluminum nitride for high temperature use.

Table 1. Material property comparison.

	Si	SiC	Al_2O_3	AlN	BeO	SiC	Borosilicate Glass	BN-hp
Density, g/cm^3	2.3	3.21	3.75	3.31	2.90	3.21	2.13	2.5
Hardness, GPa	11.5	24.0	19.0	12.0	12.0	24.0	-	2.5
Strength, MPa	250	450	350-400	350-400	200-250	450	70	53
Elastic modulus, GPa	130	470	397	320	345	420	195-265	43
Thermal conductivity, W/m·K	150	300	25	200	250	70	4.0	25
Thermal expansion coefficient, ppm/°C	3.5	3.7	7.2	4.1	8.0	3.7	3.25	0.3
Resistivity, ohm-cm	--	--	$>10^{14}$	$>10^{14}$	$>10^{14}$	1	10^{11}	10^{11}
Dielectric constant (@ 1 MHz)	11.0	42	9.4	8.9	7.0	42	4.6	4.1
Dissipation factor (@ 1 MHz)	0.09	0.05	0.0004	0.0005	0.0003	0.05	0.002	0.0045
Dielectric strength, kV/mm	--	--	15	15	10	0.7	--	--

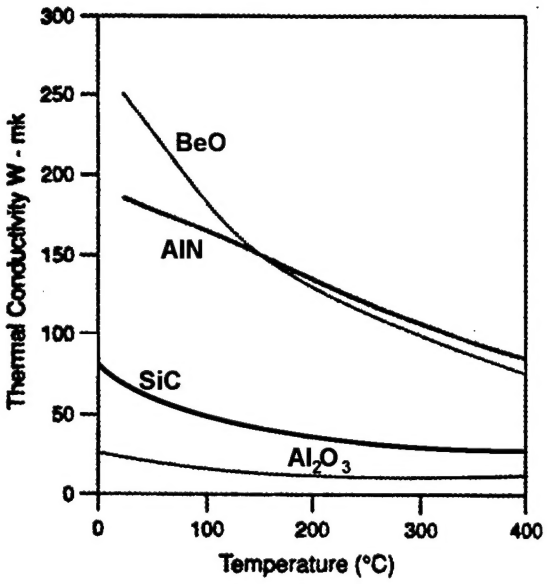

Figure 1. Thermal conductivity of commercial BeO, AlN, SiC, BeO, and Al_2O_3 (Blum, 1989).

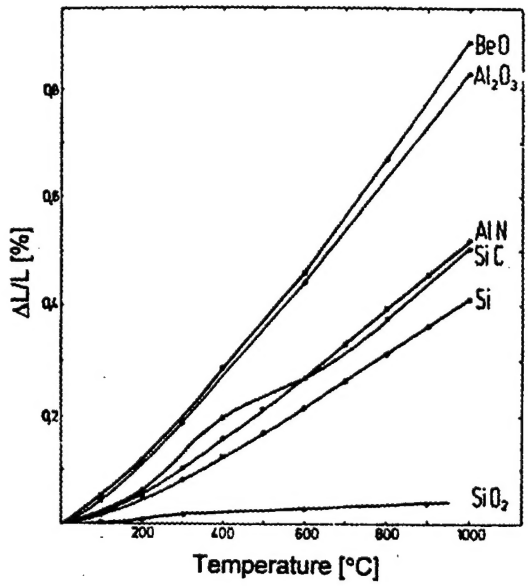

Figure 2. Thermal expansion of AlN and Al_2O_3 in comparison to that of SiC and Si (Werdecker and Aldinger, 1984).

Table 2. Dielectric constants for various materials as a function of temperature.

Material	Kr	Kt/Kr		
	23°C	1000°C	1200°C	1400°C
Fused silica (high purity)	3.82	1.02	1.03	1.04
Spinel ($MgAl_2O_4$)	8.2-8.4	1.19	1.25	--
Boron nitride	4.2-4.5	1.05	1.07	1.09
Silicon nitride	7.5-8.8	1.08	1.11	1.16
Alumina	9.5-9.8	1.15	1.21	1.27
Beryllia	6.6-6.8	1.16	1.24	1.32
Aluminum nitride	8.3-8.5	1.10	1.13	--

Table 3. Dielectric loss (tangent δ) of AlN as a function of temperature.

Temperature (°C)	Tan δ
23	0.0011
250	0.0017
523	0.0023
805	0.0050
893	0.0120
920	0.0190
950	0.022
1000	0.032

3.2 Metallization

An ideal high-temperature metallization should have high melting point, low electrical resistivity, and low-temperature coefficient of resistance, matching CTE with AlN, high bond strength between metallization and AlN, and high thermal conductivity.

Table 4 compares the relevant properties of metallic and non-metallic conductors.

Table 4. Electrically conductive materials.

Material	Resistivity (μΩ-cm)	Temperature Coefficient of Electrical Resistance ($\times 10^{3}$/°C)	CTE ($\times 10^{-6}$/°C) @ 27°C	Thermal Conductivity, (W/m·K)	Melting Temperature (°C)	Lowest Eutectic Temperature (°C)
Cu	1.5	6.8	17	398	1083	--
Au	2.0	4.0	14	315	1063	--
Al	2.4	4.29	25	237	660	--
W	4.8	--	4.5	178	3400	--
Mo	5.0	--	5.0	138	2620	--
Ni	6.0	6.9	13	91	1453	--
Co	6.2	6.04	12	100	1495	--
Pd	9.8	3.77	8.5	71	1550	--
Pt	10.6	3.9	9.0	73	1770	--
Ta	12.2	3.83	6.5	57.5	2980	--
Nb	12.5	--	7	53	2467	--
Ti	42.0	--	8.5	22	1640	--
$TiSi_2$	≈ 6.0	4.63	7.5	--	1500	1330
$CoSi_2$	≈ 6.0	--	7.5	54	1326	1195
$NbSi_2$	6.3	--	7.0	--	1950	1295
$TaSi_2$	8.5	2.24	8.3	--	2200	1385
$MoSi_2$	22	6.38	5.1	49	2030	1410
WSi_2	12.5	2.91	8.3	--	2165	1440
ZrB_2	7	2.3	7.6	58	3245	--
TiB_2	9.0	2.0	6.8	64	2980	--
NbB_2	12	--	6.5	--	--	--
ZrN	13.6	2.0	7.0	--	--	--
TiN	21.7	2.48	6.6	13	2950	--
Diamond	$>10^{9}$	--	0.8	--	--	--

3.3 Die Attach Material

From a design point of view, the ideal die attach material should have the following properties (Yang et al., 1993; Konsowski, 1993):

- Good adhesion to the die and the substrate so that the die can be attached without debonding and delamination.
- Self-resilience to provide good stress relaxation behavior so that induced internal stresses are reduced to low levels.
- High thermal conductivity so that heat dissipated from the power chip and the thermal expansion difference between the chip and the substrate can be minimized.

- An appropriate processing temperature and good thermal stability to fit into the process hierarchy such as the one shown in Figure 13.
- Corrosion resistance.
- Good reworkability.

3.4 Wires and Bond Pads

Wire material should meet the following specific criteria in addition to the general requirements given in Section 3.2 (Gehman, 1980; Tummala and Rymaszewski, 1989):

- High electrical conductivity.
- Bondability to other material with available wire bonding methods.
- Chemical compatibility with the die and substrate silicide metallization. It should not form any intermetallic compounds with bond pad metallization.
- High creep resistance to prevent sagging.
- Self-resilience to relax internal stresses, which lead to failures of wires.
- High electromigration resistance.
- High strength and ductility for plastic deformation during bonding operations.
- Be formable into fine diameters, i.e., 25 μm.
- High corrosion resistance.

4. PROGRAM DESCRIPTION

4.1 Phase II Objectives

The specific technical objectives of the Phase II research were as follows:

- To control the metal/silicon ratio to obtain stoichiometric tungsten disilicide thin films.
- To optimize the annealing process (time and temperature) to improve the electrical conductivity of tungsten silicide films.
- To measure the adhesion of tungsten silicide films to AlN substrates and to determine the effect of temperature cycling on the adhesion.
- To complete an ongoing literature survey and vendor survey to identify and select promising wire, braze, and die attach materials.
- To evaluate the brazibility and wire bondability of silicide thin films with the selected materials and to determine if an additional coating, such as Ni or Au, is needed for a successful joining process. The compatibility of the materials with each other will be investigated via accelerated high-temperature (1000-1200°C) tests and detailed microanalytical techniques.
- To extend the Phase I work to establish the compatibility of WSi_2 with SiC for chip back-side metallization.

4.2 Phase II Technical Approach

Technical approach to achieve the Phase II program objectives was as follows:

- Use two-target sputtering to co-deposit tungsten and silicon on an aluminum nitride substrate and on the back side of silicon carbide wafers, and anneal the deposited films to form stoichiometric tungsten disilicide.
- Perform a thorough literature survey to identify candidate materials for die attach, wire bonding, lid sealing, and brazing.

- Investigate W-Si-Me ternary systems to define suitable pad materials, where Me includes Cu, Au, Ni, Pd, and Pt.
- Plate tungsten disilicide films with a metal compatible with both tungsten disilicide and identified die attach and wire bonding materials to form a bond pad/diffusion barrier for die attach and wire bonding.
- Measure the adhesion between the tungsten metallization and aluminum nitride substrate by epoxy stud pull testing.
- Perform die attaching, wire bonding, and brazing, and characterize interfaces through advanced electron microscopy, including phase contrast imaging, point EDS spectroscopy, and x-ray mapping of cross section samples from diffusion couples.

4.3 Phase II Tasks

The tasks were carried out in a way that is compatible with current ceramic package production practices; therefore, the processes developed during the program are readily adaptable for commercial production. The following tasks were performed during the Phase II project.

4.3.1 Task 1. Silicide Stoichiometry Control

The objective of this task was to control the stoichiometry of tungsten silicide to minimize its electrical resistivity while maintaining a good adhesion to AlN substrate.

4.3.2 Task 2. Review Literature to Identify Wire, Wire Bonding, Die Attach, and Braze Materials

The objective of Task 2 was to conduct a literature review to identify and select wire, bond pad, die attach, and braze materials capable of continuous operation at 600°C and above and adaptable for package manufacturing unit operations.

4.3.3 Task 3. Preparation of Diffusion Couples and Experimental Verification of their Compatibility

The purposes of this task were:

- To prepare selected diffusion couples.
- To heat treat them at temperatures up to 1200°C.
- To measure relevant properties such as electrical resistivity, bond strength, and mechanical strength before and after heat treatment, as appropriate.
- To characterize interfaces via advanced electron microscopy techniques after heat treatment.

Candidate bond pad materials were sputtered or plated on W-Si metallization, as shown in Figure 3, and heat treated up to 1200°C. The adhesion of the pad on the metallization was measured by the Z-axis pull (pull stud) test. Sheet resistivity was determined by the four-probe measurement technique. Candidate wire and bond pad materials were brought into close contact to form diffusion couples at 1200°C.

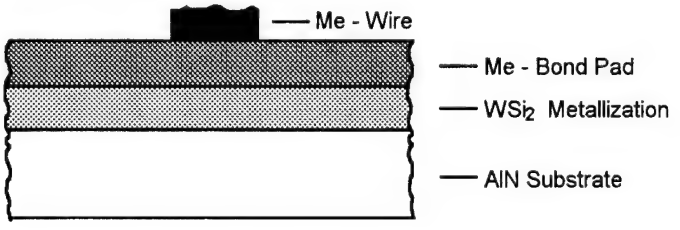

Figure 3. Compatibility test configuration for metallization - bond pad / wire system.

5. EXPERIMENTS, RESULTS, AND DISCUSSION

5.1 Task 1. Silicide Stoichiometry Control

Tungsten-silicon films were deposited on polished AlN substrates. RF magnetron sputtering was used to co-deposit the films from high purity tungsten and silicon targets. Power levels in each target were independently controlled to change Si/W ratio of the films. In addition to co-sputtering process, pure tungsten and tungsten disilicide targets were also used to deposit thin films on AlN substrates. W/Si ratio of the films were measured using electron microprobe analysis after performing calibration experiments on pure W, Si and WSi_2 samples. Sputtered W-Si films were heat treated up to 1300°C in argon and nitrogen gas atmosphere. Electrical resistance and adhesion of the films to AlN substrates were measured before and after heat treatment. Sheet resistivity was measured using 4-point probe, while high strength (> 10 ksi) epoxy bonded pull stubs were used to measure film adhesion. X-ray diffraction method was used to determine the type and the relative quantity of phases present in each film. Surface morphology and film integrity were examined before and after heat treatment using optical and electron microscopy. Transmission electron microscopy and energy dispersive x-ray spectroscopy were used to examine local chemistry of interface, W-Si film and AlN substrate.

Effect of Si/W Ratio on Properties of Thin Films

Thin films with Si/W ratios between 1.5 and 4.0 were studied. However, Si/W ratio of the sputtered films found to be lower than the compositions targeted. When WSi_2 target was used, the resulting film had a Si/W ratio of 1.17. This is not unexpected since a sputtered Si atom has a kinetic energy twice that of a sputtered W atom because of atomic weight difference between them. Therefore, the probability of Si atoms to stick to AlN surface is less than that for W atoms. Thus, the deposited film compositions are to be skewed toward W side in Si-W binary system. Si/W ratios of the sputtered films are shown in Table 5, as determined by electron microprobe analysis.

Table 5 shows the sheet resistivity and adhesive strength of the W-Si films deposited on polished AlN substrates as a function of Si/W ratio, heat treatment temperature and atmosphere. The thin films deposited from W target showed the lowest sheet resistance, regardless of the heat treatment conditions used. However, W films did not adhere well to AlN surface. Adhesion of W films was significantly improved upon incorporation of Si into W film, which also resulted in an increase in the sheet resistance. The higher the Si/W ratio of the film, the higher the sheet resistivity of as-sputtered film becomes. The same trend was also observed after heat treatment of the films, however, variation of sheet resistance as a function of Si/W ratio was not as drastic as for the case observed in as-sputtered films. Sheet resistance of the film decreased with increasing heat treatment temperature for a given composition, as shown in Table 5. This decrease of sheet resistance with heat treatment can be attributed to crystallization and grain growth in the film microstructure reducing the number of grain boundaries. The reduction of grain boundaries result in less scattering of the electrons which leads to an increase in electrical conductivity. Heat treatment atmosphere (argon versus nitrogen) did not have a significant effect on sheet resistivity of the films.

Phase compositions and crystallinity of the films were determined using x-ray diffraction analysis. All of the as-sputtered films were in amorphous state as expected. Films become crystalline upon heat treatment which also causes formation of W, W_5Si_3 and WSi_2 phases, depending on the Si/W ratio of the films. Table 6 shows the composition of the films after heat treatment, as calculated from the intensity of the peaks in x-ray diffraction data. The amount of WSi_2 increases with increasing Si/W ratio. Only one deposition process (Si/W = 1.5) yielded 100% WSi_2 film formation after heat treatment. All the other sputtered samples contained either a binary or ternary phase mixture. Films deposited from WSi_2 target also gave a 50 to 50 mixture of W_5Si_3 and WSi_2 phases, very similar to our co-sputtered film with Si/W ratio of 1.10. Furthermore, W phase formation observed in x-ray data for every films when Si/W ratio was less than 1.0.

Table 5: Electrical resistivity and film adhesion as a function of Si/W ratio and heat treatment temperature and atmosphere.

Si/W	Film Thickness (microns)	Temperature (°C)	Atmosphere	Sheet Resistance (ohms/□)	Pull Strength (ksi)
0	0.6	As Deposited	--	0.86	0.05
		1100°C	Ar	0.24	0.22
		1300°C	Ar	0.16	1.00
0.71	0.8	As Deposited	--	2.74	14.4
		950°C	Ar	1.40	--
		1100°C	Ar	0.96	3.25
		950°C	N2	1.47	--
0.98	0.8	As Deposited	--	2.58	5.9
		950°C	Ar	1.66	1.5
		1100°C	Ar	--	1.6
		950°C	N2	1.79	1.6
1.10	0.8	As Deposited	--	4.47	8.0
		950°C	Ar	2.36	11.7
		1100°C	Ar	1.50	9.4
		950°C	N2	2.39	11.4
1.5	0.8	As Deposited	--	9.90	0.2
		950°C	Ar	3.01	12.8
		1100°C	Ar	1.09	13.0
		950°C	N2	3.13	1.1
WSi_2 Target	0.2	As Deposited	--	7.22	12.4
1.17		950°C	N2	3.73	7.7
		1100°C	N2	2.50	1.95
		950°C	Ar	2.34	0.42

W-Si binary phase diagram is shown in Figure 4. Solubility limit of Si in W is not exactly known, however, silicon can have some solubility in W metal up to 4% at., as indicated by the dotted line. Furthermore, WSi_2 can only coexist with either Si or W_5Si_3 phases, but can not be coexist with W phase, per phase diagram. Therefore, the presence of three phases (W, W_5Si_3 and WSi_2) in the film with Si/W ratio of 0.98 is questionable. In this film, either the heat treatment time was not sufficiently long enough to yield thermodynamic equilibrium or W phase was not in physical contact with WSi_2 in the film structure so that the phase rule was not violated.

Table 6: Phase compositions of heat treated W-Si films as a function of Si/W ratio, as calculated from the relative peak heights in x-ray diffraction data.

	Phases present (% by weight)		
Si/W	W	W_5Si_3	WSi_2
0	100	--	--
0.71	57	43	--
0.98	37	48	15
1.10	--	51	49
1.50	--	--	100
WSi_2 target (1.17)	0	50	50

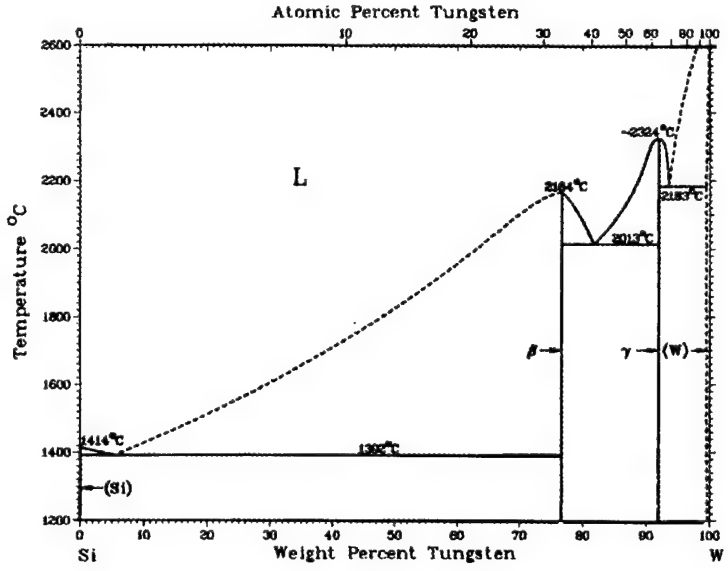

Figure 4. W-Si Binary Phase Diagram (Massalski, 1986).

Adhesion of the W-Si films to AlN substrates were measured by epoxy stud pull testing method. The method utilizes an aluminum stud that is attached to the W-Si film with a high strength epoxy. Pull test data are shown in Table 5, as a function of Si/W ratio, heat treatment temperature, and atmosphere. The data in Table 5 are not conclusive to derive a correlation between the film chemistry and adhesion strength measured. It appears that pull strength of the films decrease with increasing heat treatment temperature, with the exception of the films with Si/W ratios are 1.50 and 1.10. Thin film with ternary phase mixture (Si/W ratio is 0.98) showed the lowest pull strengths after heat treatment. This is not surprising, because thermal properties of each phase can be different due to the compositional differences, causing microstructural damage in the film to cause it to fail prematurely. Adhesive strength in as-deposited state was the highest for the film with Si/W ratio of 0.71, but adhesive strength of the film decreased after heat treatment above 1100°C.

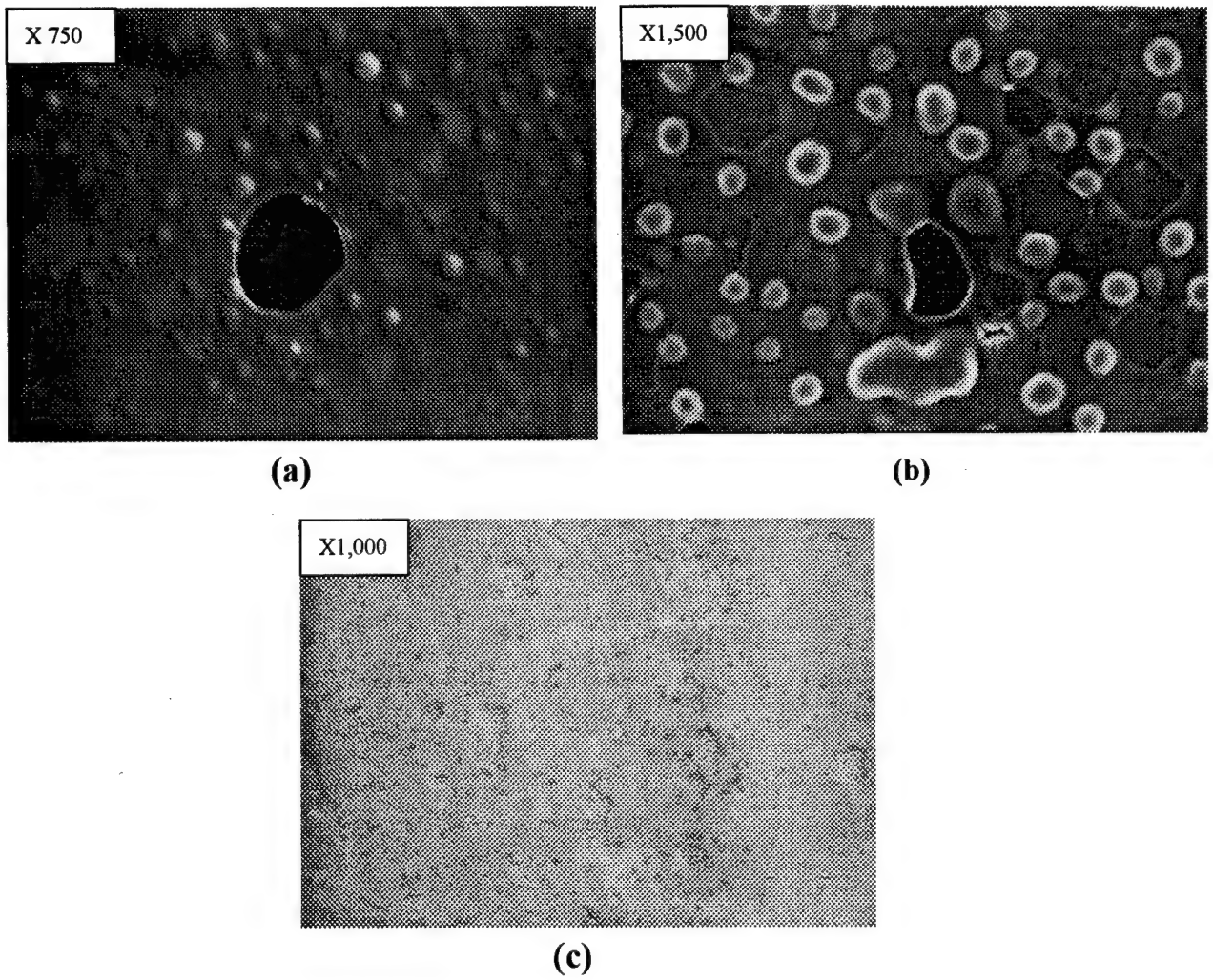

Figure 5. SEM images of W-Si Films after heat treatment at 1100°C 9a) Si/W = 1.5, (b) Si/W = 1.17, and (c) Si/W = 0.71.

Structural integrity of the films on AlN surfaces before and after heat treatment were examined using optical and electron microscopy techniques. The films survived the heat treatment process without any visible peeling, with the only exception of the sample with Si/W ratio of 0.98. This film partially cracked and peeled off from the surface after 1100°C heat treatment. Furthermore, the films with high Si/W ratios showed the presence of spherical features on the surface after heat treatment. As shown in Figure 5, these spherical features become more evident when Si/W ratio was increased. On the other hand, surface quality of the films did not show any change when Si/W ratio was 0.71. Electron microprobe analysis from the spherical features showed that these regions were silicon rich and Si/W ratio was as high as 3.4. Thus, it appears that W-Si films become structurally less stable with increasing Si/W ratio after the heat treatment. Therefore, the films with Si/W ratio of 0.71 were selected for compatibility studies between die attach, pad and wire materials.

Selection of W-Si Thin Film Composition and Its High Temperature Stability

W-Si films with Si/W ratio of 0.7 were investigated further to assess the film properties in detail before continuing compatibility study in Task 3. A number of films with a Si/W ratio of 0.7 were deposited. The sheet resistance and pull strengths are presented in Table 7 before and after heat treatment for each batch. As seen from the data in Table 7, there was a large variation in film thickness and sheet resistance in as deposited state, while pull strength of the films were generally acceptable. Variation of properties in as-deposited state suggests difficulty of control during deposition. However, variation of thin film properties became less significant upon heat treatment. After the heat treatment of up to 1300°C, neither strength degradation nor increase in sheet resistance were observed for the films. In fact, average pull strength increased slightly with heat treatment while the sheet resistance approached to the sheet resistance of pure W films, given in Table 5.

Table 7. Sheet resistivity and pull strength of samples with intended Si/W ratio of 0.71, before and after heat treatment at 1100°C in argon.

		Sheet Resistance		Pull Strength (ksi)	
Batch Number	Film Thickness (microns)	As Deposited	Heat Treated	As Deposited	Heat Treated
1	0.8	2.74	0.96	14.4	3.25
2	1.1	19.9	1.30	7.9	9.8
			0.52 *		11.9 *
3	1.5	3.92	0.4	12.5	13.1
4	1.5	5.30	0.5	11.2	12.9
5	0.8	4.8	0.9	---	---

* after heat treatment at 1300°C.

Table 8 shows the compositions of the films for different batches. The films from batches 3, 4, and 5 were identical and contained about 10% by weight W_5Si_3 and the remaining was W. Figure 6 shows the x-ray diffraction spectra of the film obtained from batch 3 after heat treatment for 30 minutes at 1100°C in argon. X-ray diffraction spectra of batch 2 showed only the presence of W phase (see Figure 7), while batch 1 yielded a 50% by weight tungsten and 50% by weight W_5Si_3 phases. The difference between the chemical compositions suggests that films did not have exactly the same Si/W ratios to start with. However, it is clear that W, which normally does not adhere to AlN, can be strongly attached to polished AlN substrates if there is a small quantity of silicon present during the sputtering (batch 2). Furthermore, having up to 10% by weight W_5Si_3 phase in the W film structure does not significantly change the electrical properties of the W-Si films.

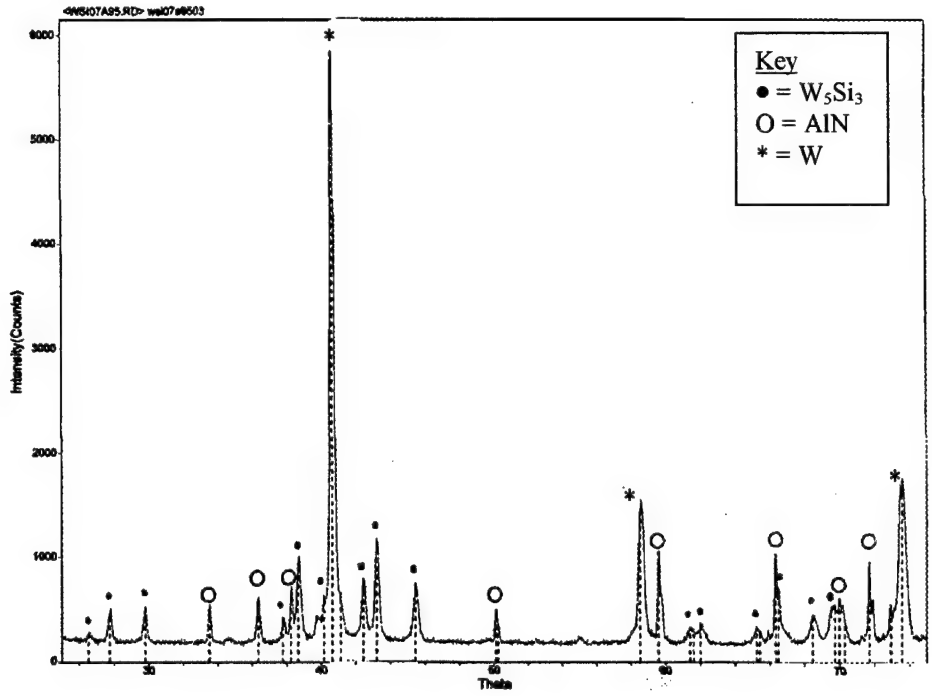

Figure 6. X-ray diffraction spectrum of the W-Si sample from batch 3, showing a mixture of W and W_5Si_3 phases. AlN peaks are from the substrate beneath the film.

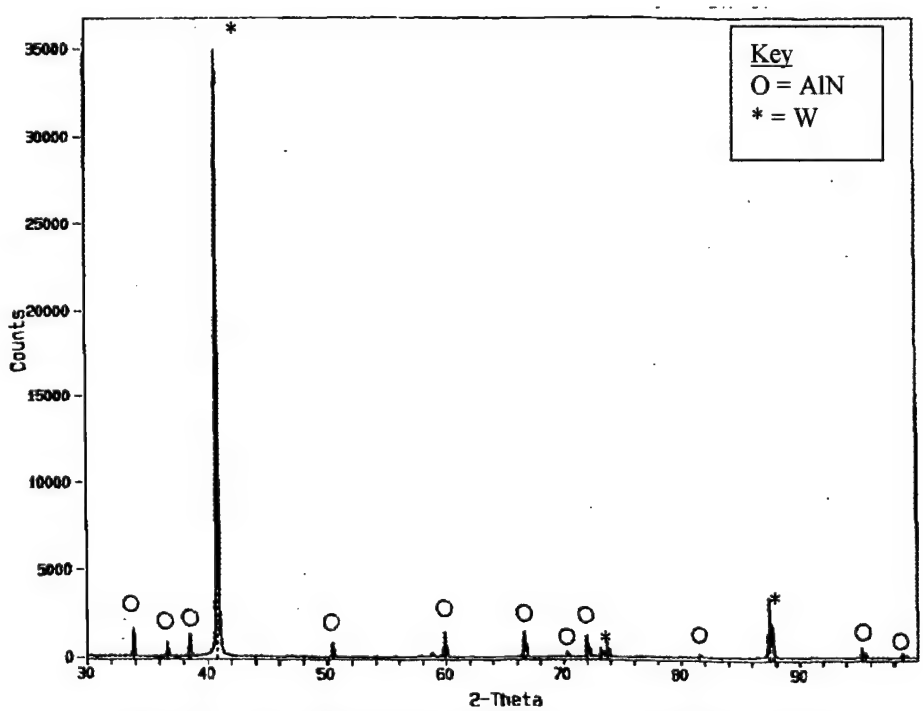

Figure 7. X-ray diffraction spectrum of the W-Si film sample from batch 2, showing only W phase in the film.

Table 8: Chemical composition of the films with intended Si/W ratio of 0.71.

Batch Number	W_5Si_3 (% by weight)	W (% by weight)
1	43	57
2	1	99*
3	10	90
4	10	90
5	10	90

* Assumed to contained maximum 1% Si since it is below the detection limit of x-ray diffraction

Long term high temperature stability and the effect of thermal cycling on the W-Si film properties were investigated for the samples prepared from the batch 3. 1.5 microns thick W-Si film was deposited on polished AlN substrate and heat treated at 1300°C up to 65 hours in argon gas atmosphere. Thermal cycle tests were performed between room temperature and 1200°C by rapid heating and cooling in a tungsten mesh heating element furnace. Heating and cooling rates were approximately 80°C/min and dwell time was 10 minutes at 1200°C for thermal cycle tests. Thermal cycle tests were performed in argon gas atmosphere and total number of cycles was 10.

Pull strengths and sheet resistances of the films before and after the heat treatment are shown in Table 9. The data in Table 9 shows there is no degradation in pull strength and sheet resistance of the films upon heat treatment at 1300°C. Sheet resistance of the films were comparable to sheet resistance of pure tungsten films (see Table 5) without any degradation of film's adhesion to AlN substrate. X-ray diffraction spectra for the film heat treated for 65 hours showed presence of some unknown peaks, in addition to the major W peaks and minor AlN peaks coming from the substrate beneath the film, as shown Figure 8. These unknown peaks neither matched the any known W-Si alloys nor any W-O compound. Although, they might originate from the second phase in the AlN substrate material, its presence did not degrade the properties of the films.

Table 9. Sheet resistance and pull strength of W-Si Film after thermal cycle and long term heat treatment. Sample is Si/W ratio of 0.71 and from batch 2.

	Sheet Resistance (Ω/□)		Pull Strength (ksi)	
Heat Treatment	As Deposited	Heat treated	As Deposited	Heat Treated
65 hrs at 1300°C	3.92	0.26	12.5	13.51
Thermal cycle to/from 1200°C	3.92	0.40	12.5	11.64

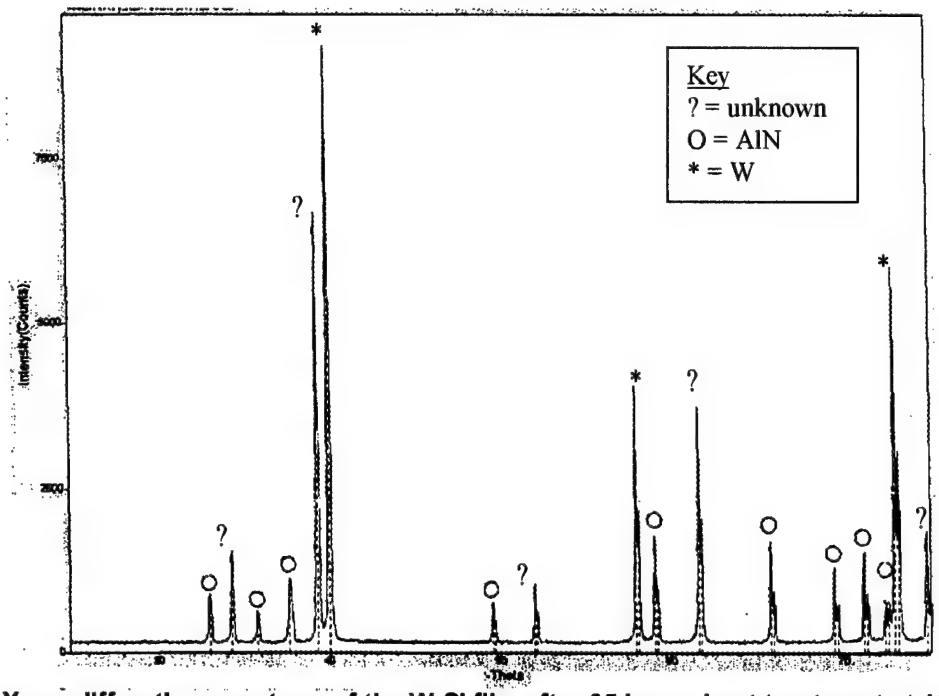

Figure 8. X-ray diffraction spectrum of the W-Si film after 65 hours heat treatment at 1300°C.

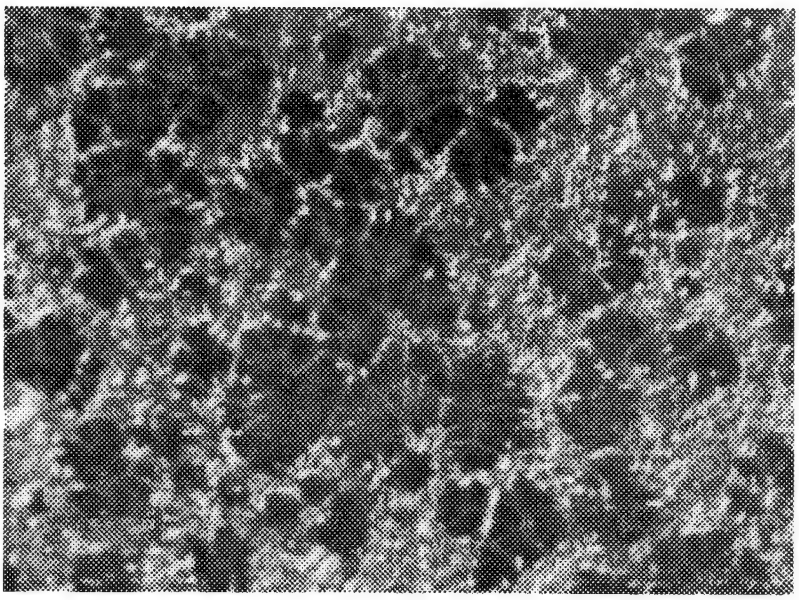

Figure 9. Dark field optical microscope image of the film surface after long term heat treatment at 1300°C.

Surface of the film after 65 hours heat treatment at 1300°C was examined using optical and scanning electron microscopy. Figure 9 shows optical micrograph of the film after the heat treatment. There appears to be a significant grain growth in the film, which may explain the lowest sheet resistance observed in this sample. Film appears to have a textured structure with two phase mixture under dark field illumination. However, backscattered electron micrograph did not reveal any contrast due to compositional

difference, suggesting only the presence of W in the film structure. Furthermore, electron microprobe analysis of various locations on the film surface only showed W, suggesting there was no contamination from the AlN substrate beneath the film. Despite the fact that we could not determine clearly the nature of additional phase in the films after 65 hours heat treatment, the film appeared to be stable after excessive heat treatment conditions.

Transmission Electron Microscopy of the Thin Film/AlN Interface

Interfaces between AlN and W-Si film (Si/W = 0.71, batch 2), and between AlN and pure W film were examined using transmission electron microscopy (TEM). Cross-sectional electron transparent TEM specimens were prepared to perform structural and chemical analysis of the film, AlN substrate, and the interface. Thin film samples were cut across the substrate thickness and film containing surfaces were glued to each other using electrically conductive and radiation resistant epoxy. Sample was mechanically ground to decrease its thickness to less than 100 microns, then thinned further in ion beam milling machine to make it electron transparent at low temperature (liquid nitrogen) to prevent beam damage. The final sample thickness was in the order of 0.1 microns.

Figure 10 shows the bright field image taken from the pure W film-AlN interface. As seen in the figure, pure W film did not adhere to AlN. Energy dispersive x-ray spectroscopy across the interface did not reveal any evidence of W diffusion into the AlN structure.

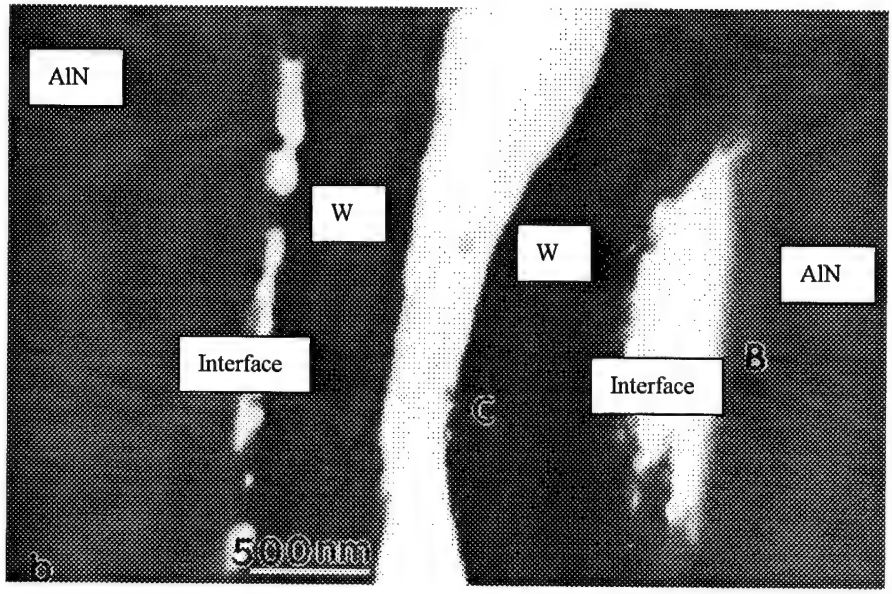

Figure 10. Bright field TEM image of W-AlN interface, showing lack of adherence of the W film to the AlN substrate.

Figure 11 shows the bright (a), and dark field images (b) taken across the interface of the sample with W-Si film deposited and heat treated at 1100°C (batch 2 with Si/W ratio of 0.71). The presence of Si in W film improved the adhesion of the film to AlN substrate, as also illustrated by the pull test results in the previous section. No detached regions were observed across the interface. Epoxy region in bright field image is designated as E and cross-section is repeated on both side of the epoxy region, per sample preparation method used. Both AlN and W-Si film regions appear to be uniform, while W-Si film region displays polycrystalline character, AlN region displays a large single crystal on each side. One prominent feature across the region from W-Si film into the AlN is the presence of a lighter band region, indicated as TR.

This light banded zone is called as transition region (TR) and its composition and structure is investigated in detail below.

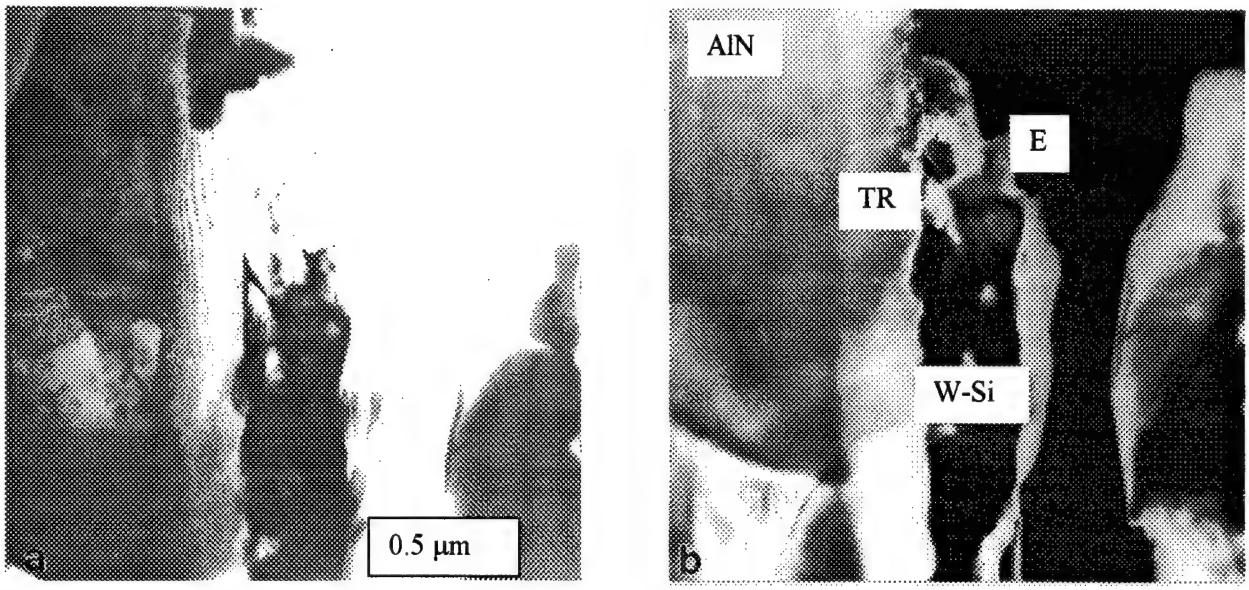

Figure 11. Cross-sectional TEM images taken from the W-Si sample obtained from batch 2, after heat treatment at 1100°C. (a) Bright field and (b) dark field images.

Microstructure and local chemistry of the interface region were analyzed using micro diffraction and energy dispersive x-ray spectroscopy methods. For ease in analysis in the diffraction experiment, the sample was tilted so that the AlN matrix would give a zone axis pattern. Figure 12 (a) shows the locations where microanalysis was performed in a bright field TEM image. As shown in Figure 12 (b), micro diffraction patterns from locations 2 and 3 are very identical to each other, indicating that the TR region has a similar crystalline structure as AlN. From the diffuse nature of the diffraction discs, it is concluded that the TR region contains high density of lattice defects. Diffraction pattern taken from location 1 gave a superposition of several micro diffraction patterns, all originating from the W (bcc) crystals.

Energy dispersive x-ray spectra taken from locations 1, 2, and 3 are shown in Figure 12 (c). Copper peak (8.5 kV) observed in spectra is from the background. As expected, location 1 is mostly composed of W phase. On the other hand, locations 2 and 3 contain mostly Al peaks, associated with AlN phase. However, location 2 also shows a small peak at 1.8 kV, associated with Si. Therefore, it can be concluded that Si diffuses into the AlN in the TR region.

At the end of the Task 1, Si/W ratio 0.7 was selected for metallization of AlN substrates for compatibility studies planned for Task 3. This decision was based on the following reasons; films not only survived high temperature heat treatment process with good film integrity and high pull strength, but also displayed lowest sheet resistance. Compositions that yielded pure WSi_2 film formation and/or multi phase mixtures were not stable in terms of film stability, also presented adhesion problems to AlN surfaces. Therefore, for the rest of the study, compositions prepared from batches 3, 4, and 5, shown above in Table 7, were used to investigate the compatibility of die attach, pad, braze and wire materials with the W-Si films deposited on AlN surface.

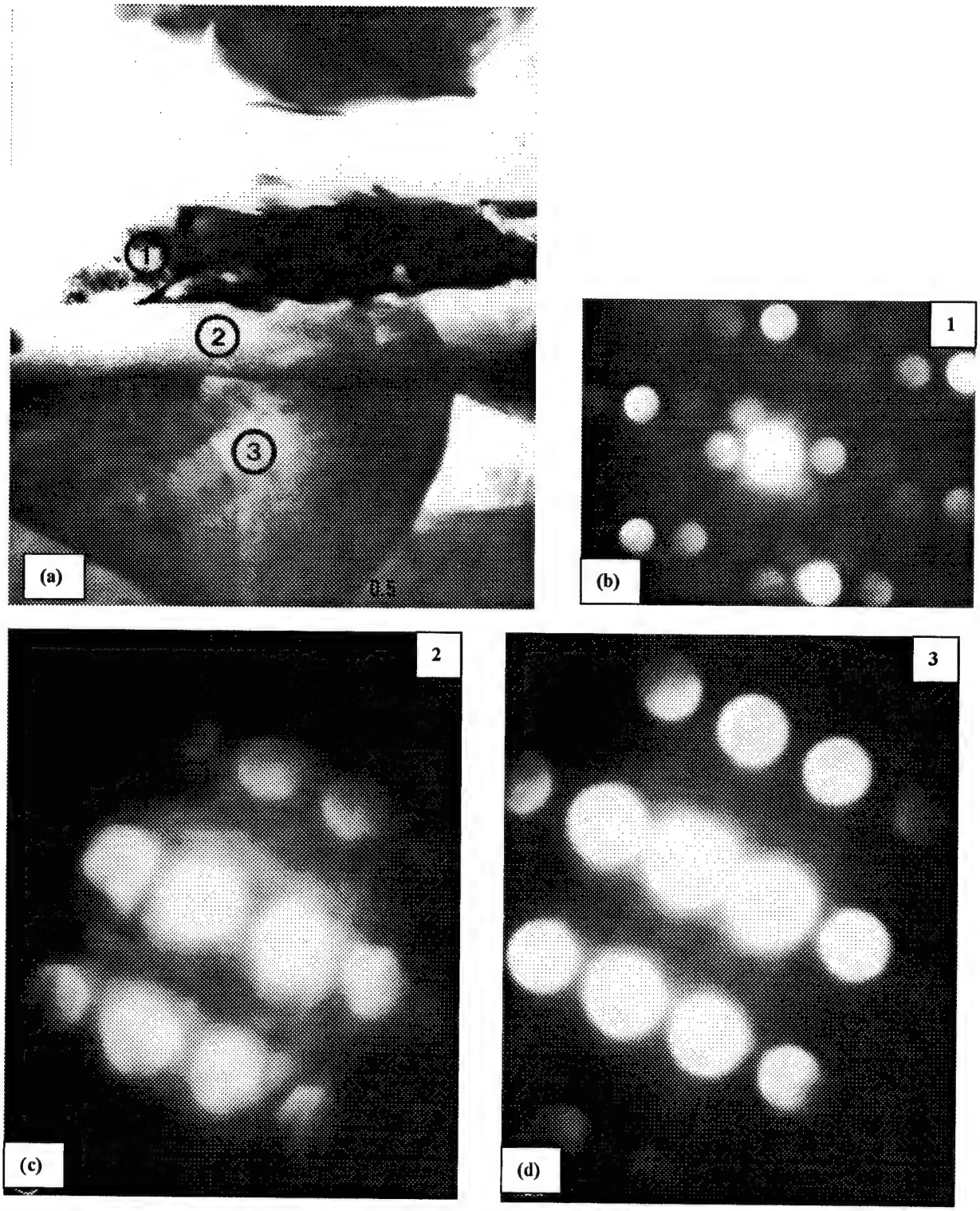

Figure 12. (a) Structural and compositional analysis locations in the W-Si/AlN cross-section, (b,c,d), micro diffraction patterns taken from those regions, and (e,f,g) EDS spectra obtained from the same locations.

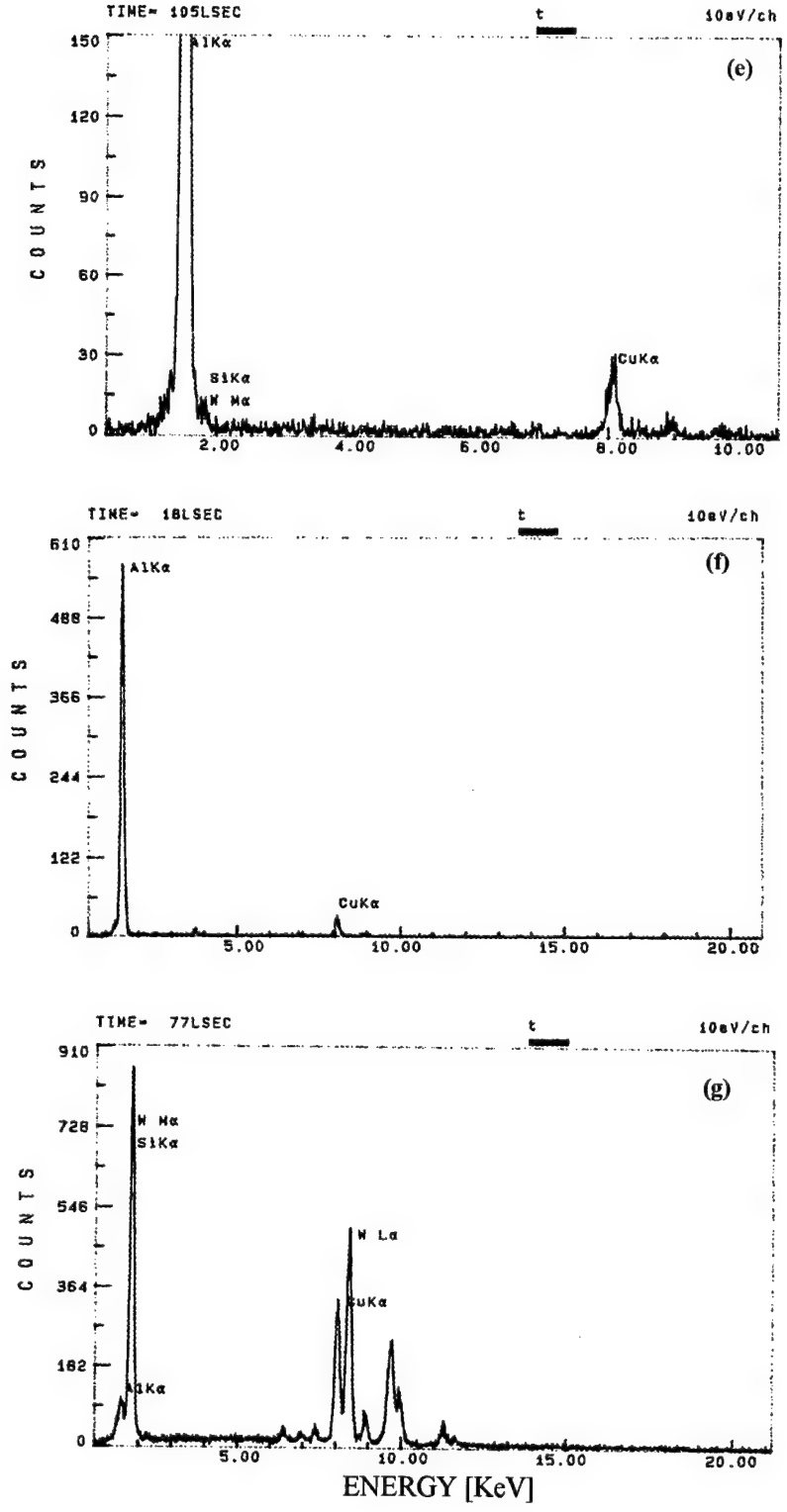

Figure 12. (Continued) (a) Structural and compositional analysis locations in the W-Si/AlN cross-section, (b,c,d), micro diffraction patterns taken from those regions, and (e,f,g) EDS spectra obtained from the same locations.

5.2 Task 2. Review Literature to Identify Wire, Wire Bonding, Die Attach, and Braze Materials

The purpose of this task was to select suitable materials that can be used as die attach, bond pad, and wire. These materials will not only be coupled with W-Si metallization film selected in the previous task, but also will be coupled with SiC die for continuous operation temperatures of 600°C and above. This high temperature requirement limits the number of available materials.

In selecting materials for interconnection, the following general rules were observed:

- The melting temperature of the metal should be at least 1.5 times higher than the operating temperature to prevent any diffusion-related problems such as creep and electromigration; and because atomic diffusion becomes significant at $T = 2/3\ T_m$ in metals.
- The metals in contact with each other should not form intermetallics at operating temperatures.

The reactivity of the metal, electromigration, grain growth, and hillock growth are influenced by the self-diffusion in the metal and between the metal and its surroundings. Diffusion in metals is related to the melting point and the crystallinity of the metal. The higher the melting point, the lower the diffusivity. The self-diffusion in a metal is related to its melting point by the following empirical relationship:

$$Q_{SD} = 34T_m$$

where Q is the activation energy in calories per mole and T_m is the melting point in degrees Kelvin. In package construction, all materials used must have melting points well above 600°C. The materials must also have a hierarchy of melting temperatures, as shown in Figure 13, that permits the desired sequence of assembly, i.e., die attachment then sealing and lid attachment. However, this hierarchy does not need to be rigid, because some attachment steps may involve only local or transient heating.

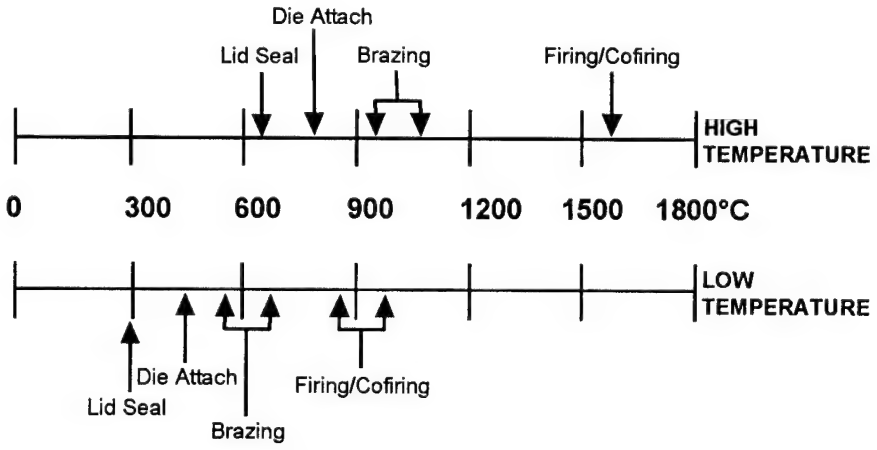

Figure 13. Schematic of process hierarchy in packaging systems.

Copper, gold, and nickel appear to satisfy this criterion when their melting points are considered. While Cu and Au can be used up to 700°C, Ni could be used up to 950°C. Palladium and platinum are other metal candidates that can be considered as interconnect material, meet the above criterion up to 1050°C, in the expense of higher cost. Since it was shown in the previous section that W-Si films can be used as a stable

high temperature metallization material on AlN substrates, compatibility of Cu, Au, Ni, Pd, and Pt with W-Si metallization and with each other should be investigated. This forms the basis for the next task in this project.

A literature survey was conducted to evaluate the phase diagrams available on the subject under this task as a starting point. Since there were no W-Si-Me ternary phase diagrams available, therefore, we utilized binary diagrams whenever available.

Currently available phase diagrams in Ni-W and Pd-W binary systems do not indicate the presence of any low temperature eutectic composition, but some intermediate alloys are likely to form during operation at elevated temperatures, as seen from the phase diagram shown in Figure 14. This is especially true for the Ni-W system, since two intermediate phase formation is possible as low as at 600°C. Thus, nickel is likely to react with W-Si films. On the other hand, Pd could be a good candidate for pad and wire applications since Pd-W phase diagram does not show any intermediate phase formation. However, it reactivity with W-Si film may be different in the presence of Si. Therefore, experimentation was necessary to determine the reactivity of Pd with W-Si films of interest.

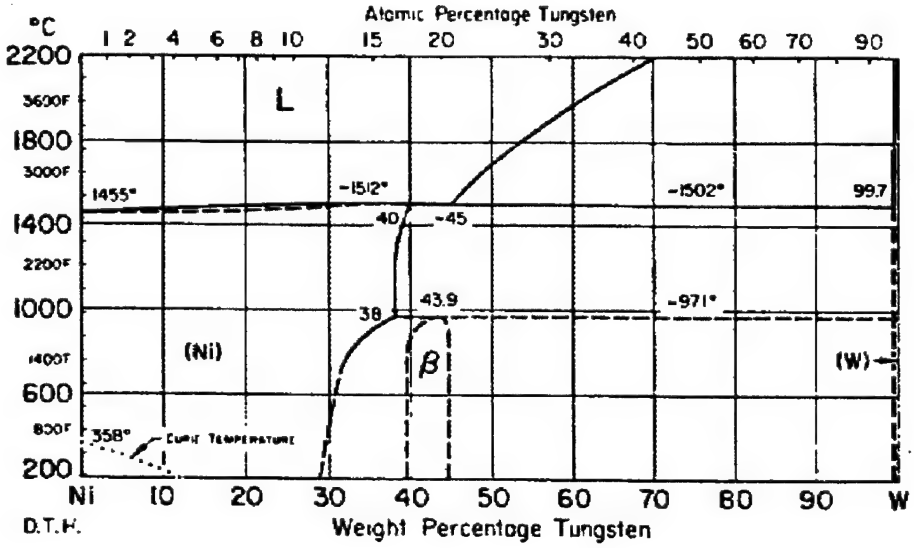

(a)

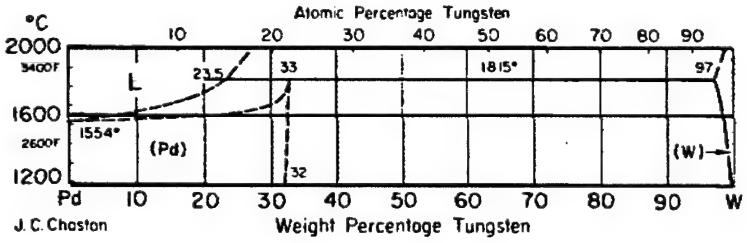

(b)

Figure 14. Binary phase diagrams of (a) Ni-W, and (b) Pd-W systems (Metals Handbook, 1973).

There is no clearly defined phase diagram available in Cu-W, Au-W and Pt-W binary systems. The available ones are speculative in nature and are shown in Figure 15. These speculative phase diagrams suggest that there should not be any reaction between W and related metals (Cu, Au or Pt). If this is true, then, Au, Cu and Pt can be used in high temperature packaging applications for operations temperatures of 600°C and beyond. Experiments were conducted in next task to determine whether this is true or not, especially in the presence of Si in the film composition.

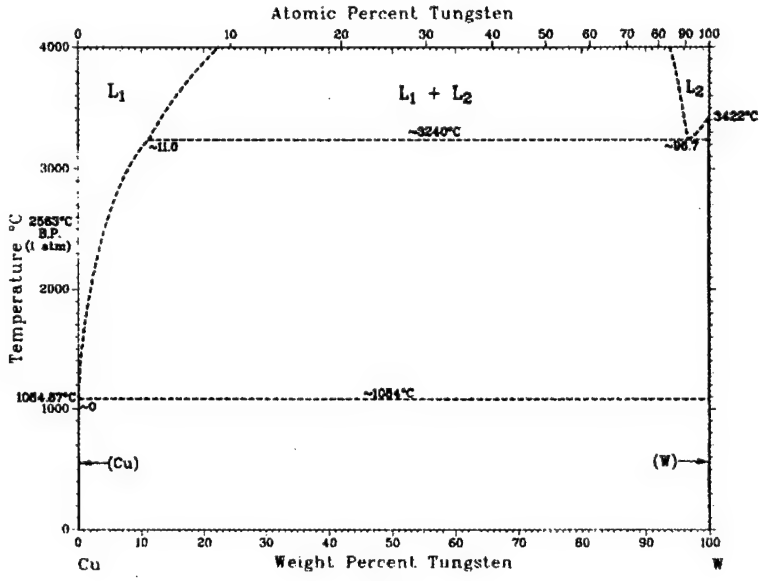

(a)

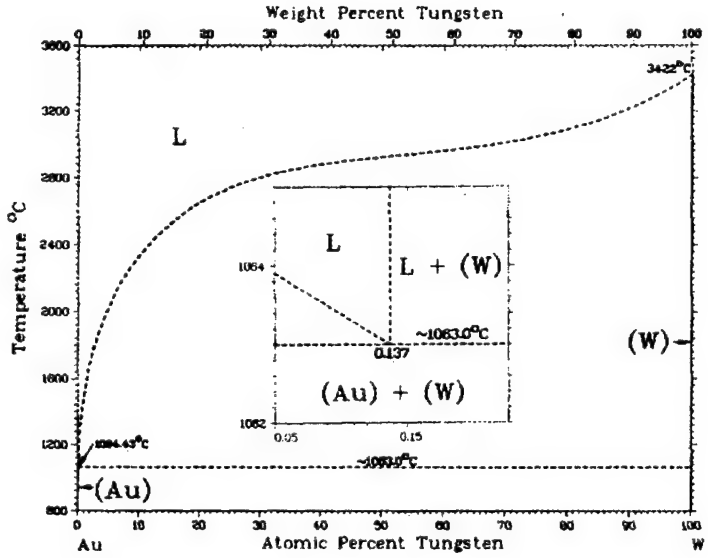

(b)

Figure 15. Binary phase diagrams proposed for the systems of (a) Cu-W, (b) Au-W, and (c) Pt-W (Massalski, 1986).

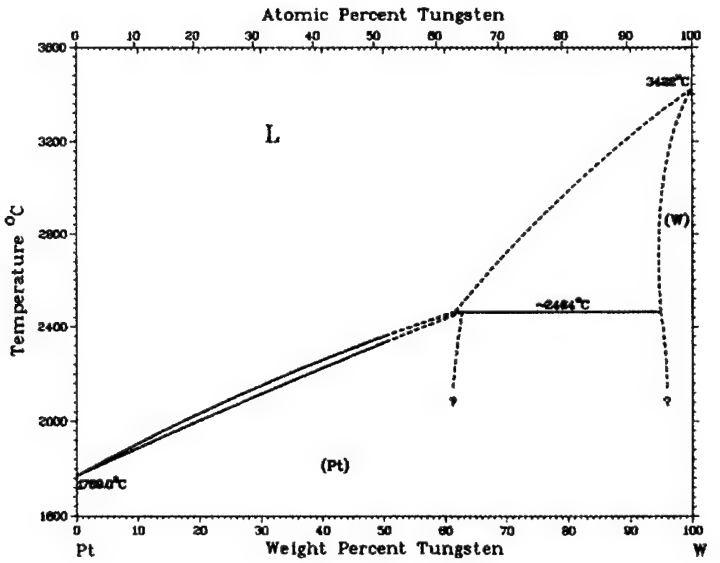

(c)

Figure 15. (Continued) Binary phase diagrams proposed for the systems of (a) Cu-W, (b) Au-W, and (c) Pt-W (Massalski, 1986).

The metals mentioned above can be used for both a pad and wire connection, therefore, foil and wire forms were considered in compatibility studies with W-Si films.

Commercially available high temperature brazing alloys were considered as a die attach material. After consulting with various vendors on the subject, four type of brazing alloys were selected to study compatibility with SiC die and with W-Si films. Compositions of these alloys and their properties are shown in Table 10.

Table 10. Compositions and properties of die attach materials considered.

Trade Name* / Property	Nicoro	TiCuNi	Copper-ABA	Gemco
Composition (%)	62Cu-35Au-3.0Ni	70Ti-15Cu-15Ni	92.8Cu-3Si-2.2Ti-2Al	87.9Cu-11.8Ge-0.3Ni
Liquidus Temp (°C)	1030	960	1024	975
Solidus Temp (°C)	1000	910	958	880
Density (g/cm^3)	10.9	---	8.1	8.82
Thermal Conductivity (W/m•K)	70	---	38	24.3
Thermal Expansion Coeff. (RT-500°C)	17.8×10^{-6}	20.3×10^{-6}	19.5×10^{-6}	---
Electrical Resistivity (Ω•m)	110×10^{-9}	---	198×10^{-9}	311×10^{-9}
Yield Strength (MPa)	185	---	279	117

*WESGO Metals Division, Belmont, CA

Monometallic systems meeting above criteria make excellent high temperature wire interconnections. Au-Au and Pt-Pt couples should provide highly reliable high temperature operation. They can be bonded using conventional wire bonding methods. Cu-Cu and Pd-Pd systems can also operate at high temperatures if the oxidation issues can be resolved. However, Pd wire bonding may require parallel-gap electrode welding due to its high hardness. Bi-metallic systems present an extra level of difficulty due to differential diffusion. Figure 16 shows diffusion coefficients of gold in the metals being considered for interconnections. The diffusion data in Figure 16 were used in selecting Au-based bimetallic systems.

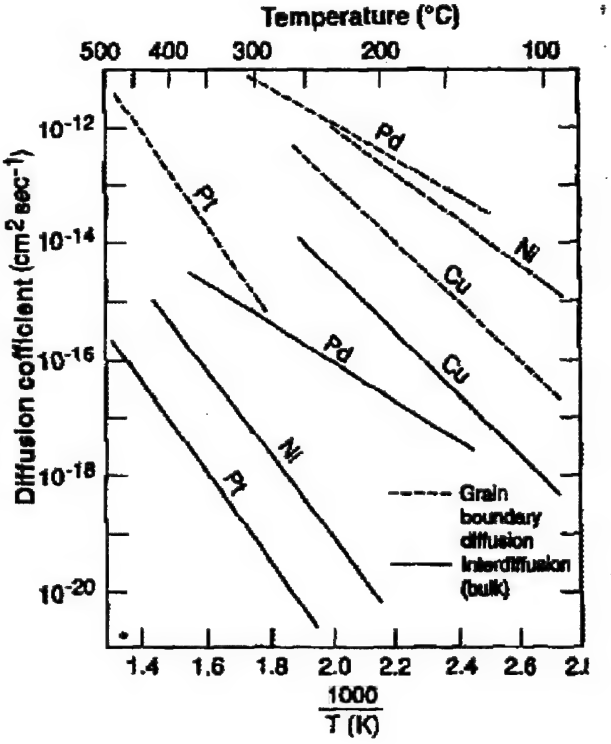

Figure 16. Diffusion coefficients for diffusion couples with gold as the top layer (Hall and Morabito, 1978).

5.3 Task 3. Preparation of Diffusion Couples and Experimental Verification of their Compatibility

The purpose of this task was to investigate the compatibility of the W-Si films with the selected braze, pad, and wire materials mentioned in the previous task. In the experiments, W-Si thin films with Si/W ratio of 0.71 from the batches 3, 4, and 5 were used. Composition and properties of these batches were identical to each other so that no other variable is introduced to experiments other than temperature and candidate material type used.

Compatibility Studies between Candidate Pad Materials and W-Si Films on AlN Substrates

1) Au-W system

About 1.0 micron thick gold layer was sputtered on top of W-Si film. Pull strength of the gold film was measured as-deposited and found to be less than 3 ksi. Failure occurred from the Au-W interface suggesting Au did not adhere to W well (Figure 17 (a)). Heat treatment of the sample at 700°C for 3 hours in argon caused gold film to partially peel off the surface (Figure 17 (b)). Optical micrograph of polished

cross-section, as shown in Figure 17, showed that gold did not adhere to W-Si surface unless an adhesion layer was used before gold deposition. Thus, a thin (about 100 Å) chromium adhesion layer was used to couple gold coating with W-Si film. As seen in Figure 17 (c) and (d), gold-W interface was intact in as-sputtered and after heat treatment steps. Pull test strength of the gold layer did not changed after heat treatment at 700°C, displayed pull strength value higher than 12 ksi. Examination of pull tested fracture surface in SEM, supplemented with electron microprobe analysis in various regions, indicated that failure occurred partially from W-Si film/AlN interface, but mostly from the epoxy/Au interface.

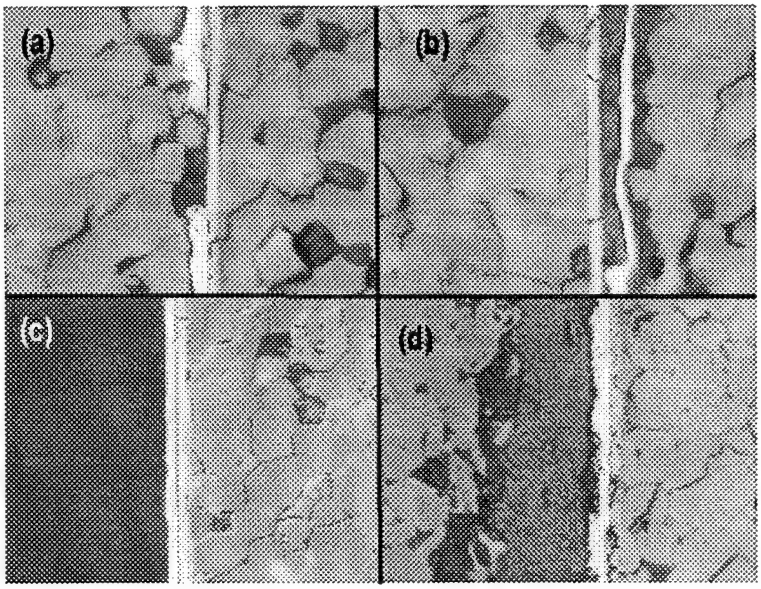

Figure 17. Optical microscope images of the polished W-Si/Au interfaces without Cr adhesion layer (a) before and (b) after heat treatment at 700°C; and with Cr adhesion layer (c) before and (d) after heat treatment at 700°C.

Sheet resistance of the Au on W-Si films increased from 0.06 ohms/□ to 0.11 ohms/□ after the heat treatment at 700°C. Increasing sheet resistance could be due to the reaction of Cr bonding layer with W-Si film and/or gold layer. Electron microprobe analysis was performed across film cross-sections using polished edges. Both as deposited and heat treated samples were used for the microprobe analysis. Figure 18 shows the backscattered electron (BSE) image of as deposited gold on W-Si film and EDS spectra taken across the film thickness. From the contrast of BSE image, there are three different zones present in as deposited film: region (a) is pure gold, region (b) is a mixture of gold and W with presence of Cr bonding layer and region c contains only W element, corresponding to W-Si film on AlN surface. Figure 19 shows BSE images and EDS spectra taken from the same sample and regions after heat treatment at 700°C. As seen, Cr peak is no longer present any specific location across the film thickness. Since Cr concentration was small in the film, it is possible that during heat treatment it diffused homogeneously through out the W-Si film coupled, so that its local concentration decreased below the minimum detection limit of electron microprobe method. Thus, increasing sheet resistance of the gold film may be due to the solid solution formation with presence of minor chromium. Nevertheless, gold appears to be a good candidate as a pad material to be used with W-Si metallized layer on AlN substrates since its pull strength and sheet resistance do not significantly change after heat treatment at 700°C.

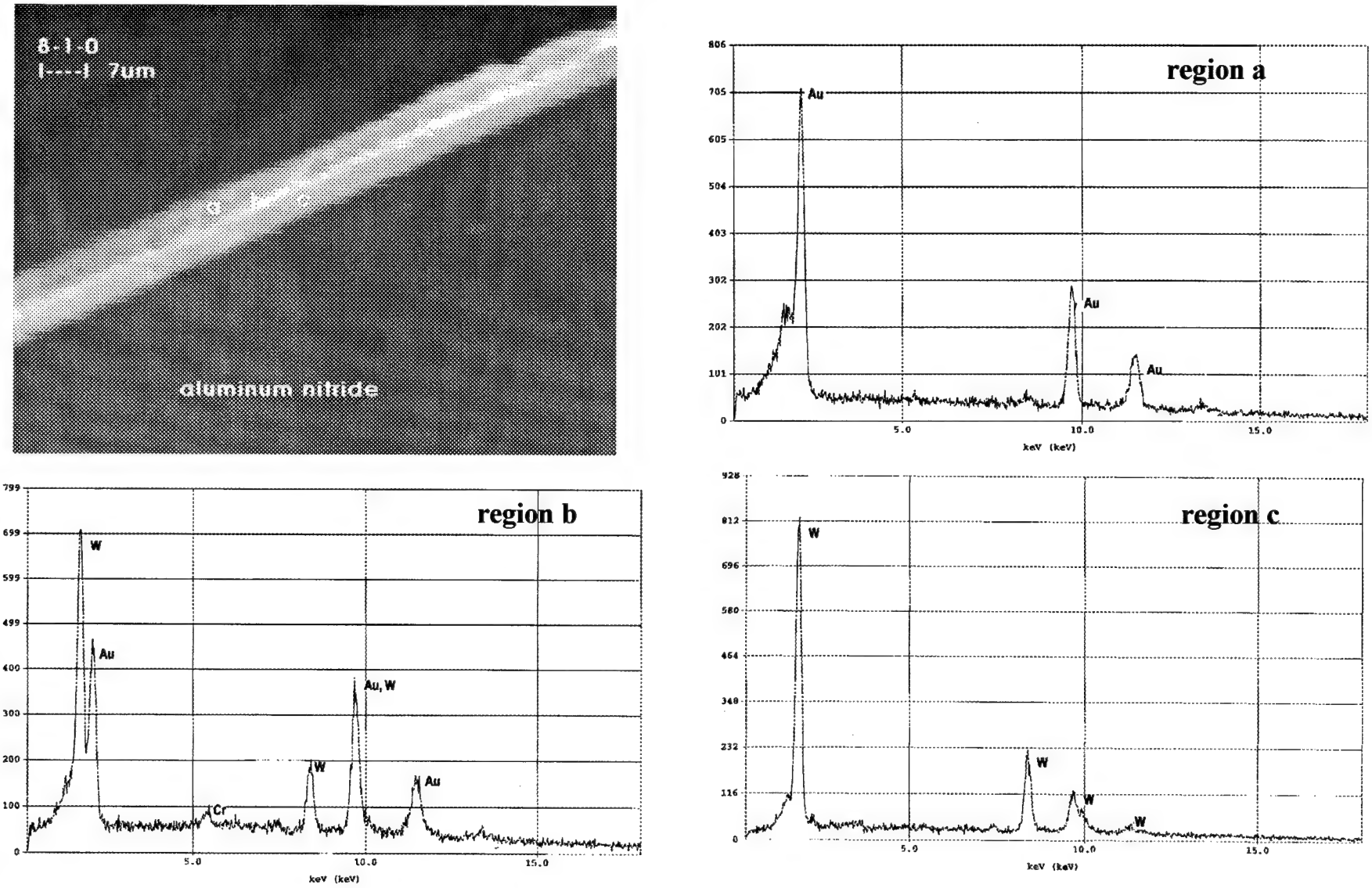

Figure 18. BSE image and EDS spectra from locations across the as-deposited Au-W film on AIN substrate.

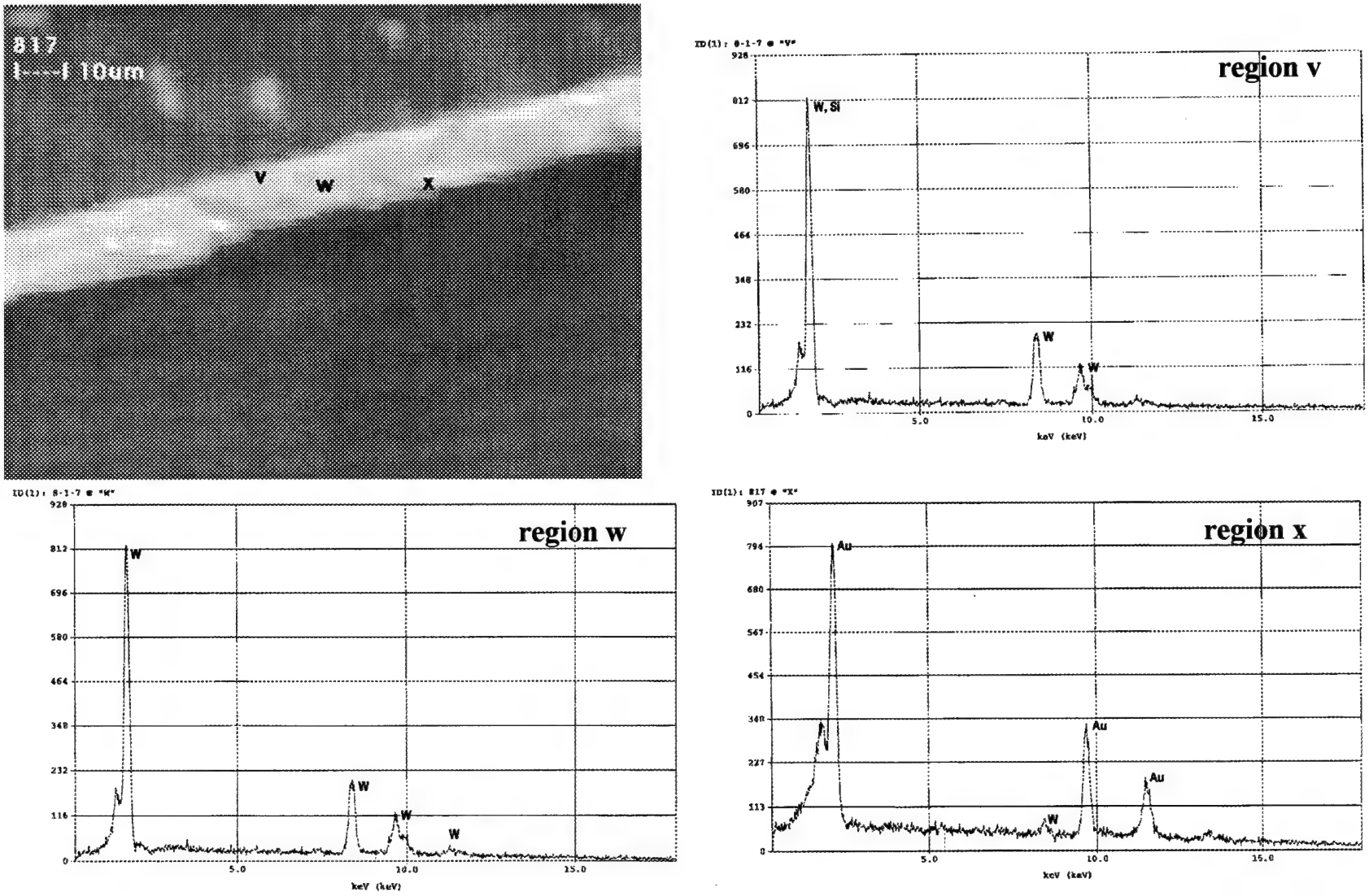

Figure 19. BSE image and EDS spectra obtained across the Au-W film on AlN substrate after heat treatment at 700°C.

2) Cu-W system

Two types of sample preparation methods were used to investigate the compatibility between Cu and W-Si films for temperatures up to 950°C. In the first approach, 25 micron-thick copper foil was paired with crystalline W-Si film deposited on an AlN substrate. The assembly was heat treated at 950°C for one hour in argon gas atmosphere. In the second approach, 1 micron-thick copper layer was sputtered on top of crystalline W-Si film. 10 Å-thick Cr adhesion layer was applied on W-Si film before sputtering of copper. The thin film pairs were heat treated in argon at 700°C for 3 hours. Pull strengths and sheet resistance of the films were measured before and after the heat treatment.

After heat treatment of copper foil/ W-Si film assembly at 950°C, copper foil was weakly attached to W-Si film with pull strength of less than 1 ksi. Figure 20 shows the region of W-Si film where most of the attachment occurred between copper and W film. Remaining copper foils are visible on the film surface after removal of the copper foil. This experiment was repeated twice using W-Si films from batches 4 and 5. In both cases, the same results were obtained (i.e. copper slightly attached to W-Si foil). Electron microprobe analysis was performed on one of the W-Si film surface after removal of the copper foil. Microprobe analysis was done not only in the region where copper was in contact with the W-Si film, but also outside the immediate contact area. Presence of copper was detected in every region examined, in addition to W and Al elements, coming from the W-Si film and AlN substrate beneath the film, respectively. Thus, it appears that copper can diffuse into the W-Si film, not only in the contact region, but also laterally throughout the film surface. This is an interesting finding since copper and tungsten are not expected to react with each other. Per the phase diagram presented in the previous section (see Figure 15(a)). It is possible that either reactivity of tungsten is being activated with the presence of silicon in the film structure (similar to improved adhesion of W-Si film to AlN substrate with presence of Si in the film), or self diffusion of copper is enhanced due to high (i.e., 950°C) heat treatment temperature used.

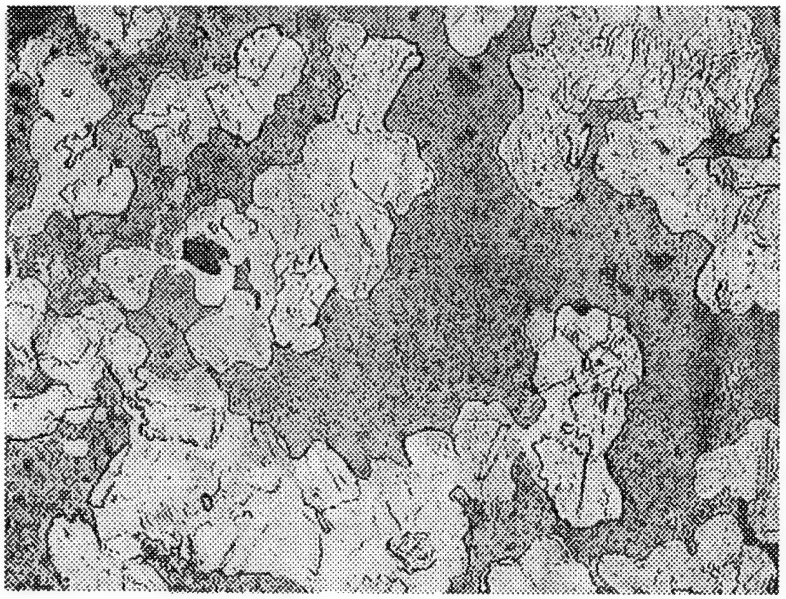

Figure 20. Optical microscope image of the W-Si surface after removal of copper foil which was in contact with W-Si film at 950°C for one hour. Copper fragments stuck to W-Si surface suggesting local interaction between W-Si film and copper foil.

About 1.0 micron-thick copper film was sputtered on crystalline W-Si film and heat treated at 700°C and 400°C in argon gas. A 10 Å-thick Cr adhesion layer was applied between W-Si film and copper. Pull strength and sheet resistance of copper film were measured as 12 ksi and 0.06 ohms/□, respectively. Pull tested stud and W-Si film surfaces were examined in SEM and determined that fracture occurred through the epoxy/Cu and W-Si/ AlN interface. There was no evidence of failure at the Cu/W-Si interface in as-sputtered copper film, suggesting a strong bonding at the Cu/W-Si interface with the presence of chromium. Cross-sectional electron microscopy and EDS analysis were performed on polished cross-sections. As shown in Figure 21, W was the only element present in the film region next to AlN surface, but the presence of W still detected towards to copper film surface. Heat treated film (at 700°C) also showed a similar elemental distribution throughout the sample cross-section. Upon heat treatment of the films at 700°C, sheet resistance of the films increased to 0.24 ohms/□ while the film pull strength dropped to 7 ksi strength level. Copper surface become blue colored, indicating some reaction in the presence of chromium. Heat treatment at 400°C did not cause any pull strength degradation and color change in copper film.

It appears that W-Si film reacts with pure copper foil at 950°C, while strong reaction occurs at 700°C when chromium adhesion layer was used between W-Si film and copper. On the other hand, copper appears to be stable up to 400°C in contact with W-Si film when chromium adhesion layer is used. Therefore, copper can be used up to 400°C safely as a pad material, but not recommended for temperatures higher than 400°C.

3) Ni-W System

Compatibility between Ni and W-Si films were investigated up to 900°C since a eutectoid reaction occurs approximately at 970°C, based on the available phase diagram shown in Figure 14 (a). The phase diagram also suggests that Ni and W are expected to react with each other to form Ni-W intermetallic phase. If this is true, then, nickel is not a feasible pad material in contact with W-Si thin film at high temperature applications.

Nickel film (20 microns thick) was deposited on crystalline W-Si film by electroplating. On top of nickel, 20 micron thick copper foil was placed to simulate the position of copper wire against nickel pad material. Samples were heat treated for 0.5 and 2 hours at 750°C, while for 1 hour at 900°C. Figure 22 shows the W-Si film surface after 900°C heat treatment. In all cases, nickel reacted very aggressively with W-Si film, consumed the W layer and leaving behind AlN surface, especially in those region where there was an intimate contact between Ni and W-Si layer. Similar reaction occurred as low as at 750°C after 0.5 hours of heat treatment. Electron microprobe analysis performed on various region of the samples confirmed that Ni consumed W-Si film, as indicated by Ni-W phase diagram (see Figure 14 (a)). Region 1 in Figure 22 only showed the presence of Al peaks, while regions 2, 3 and 4 showed the presence of Ni and Copper, in additions to major W peaks. Therefore, nickel can not be used as a potential pad material in high temperature packaging applications if the proposed W-Si film is to be used as metallization layer on AlN substrates.

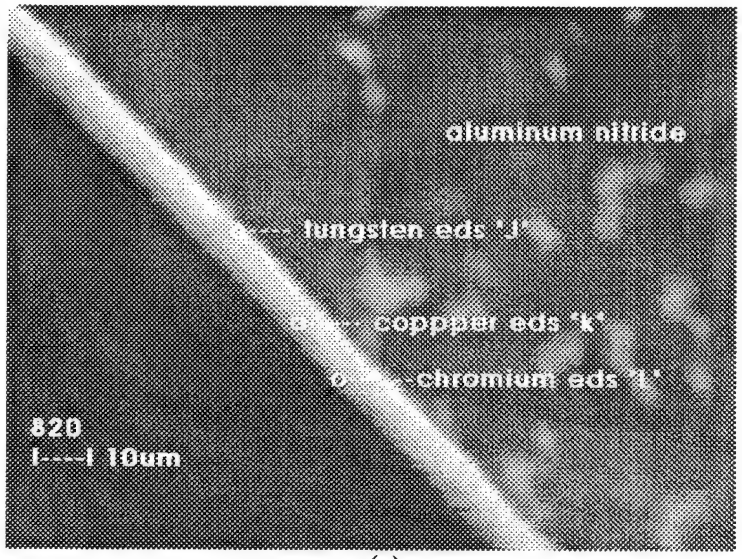

(a)

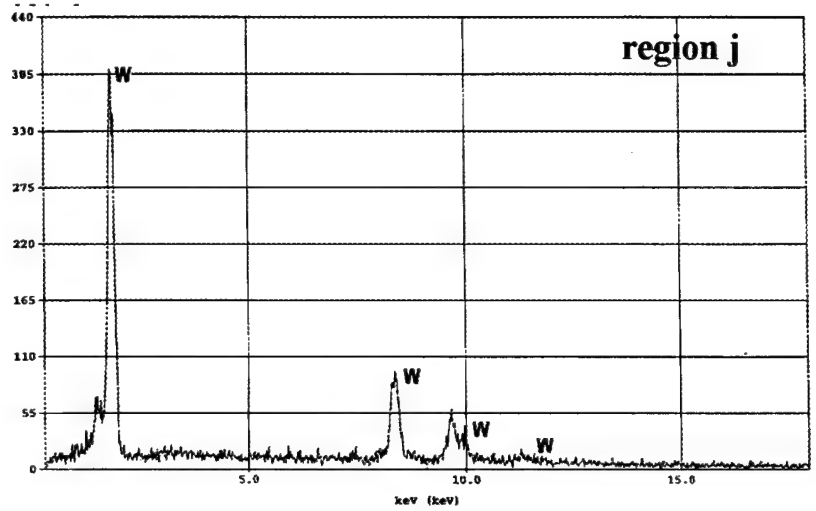

(b)

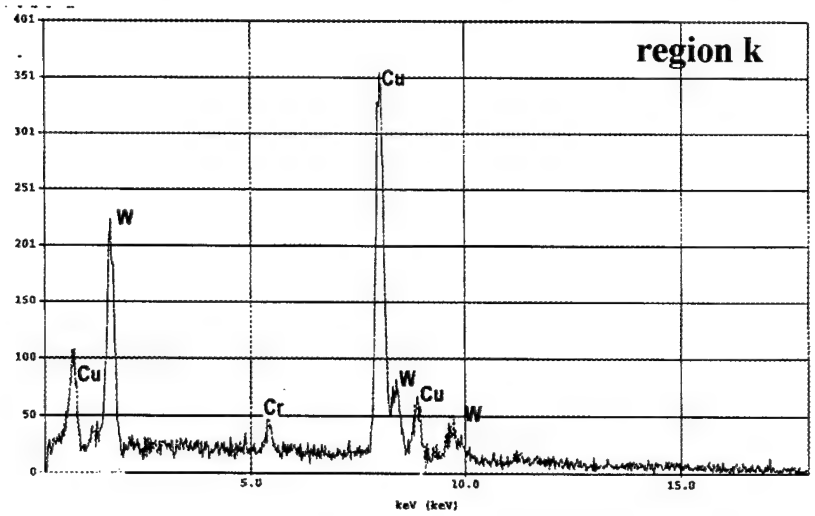

(c)

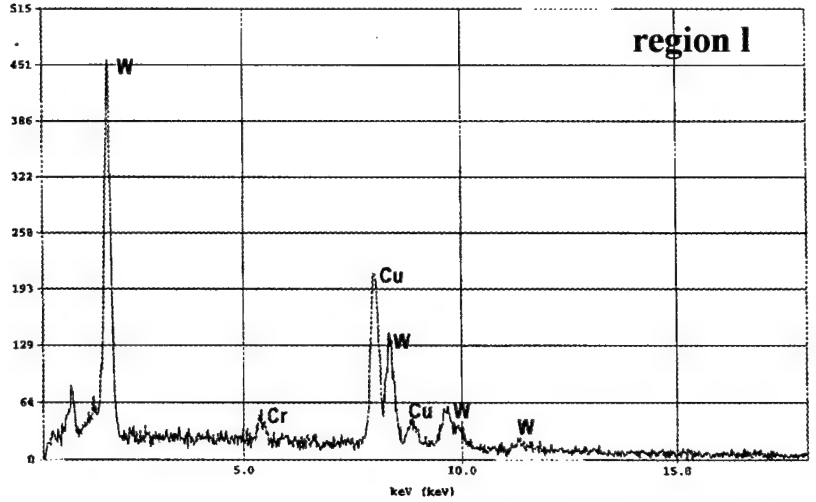

(d)

Figure 21. Cross sectional electron microprobe analysis of as-sputtered Cu/W-Si film interface (a) BSE image and (b,c,d) EDS specta.

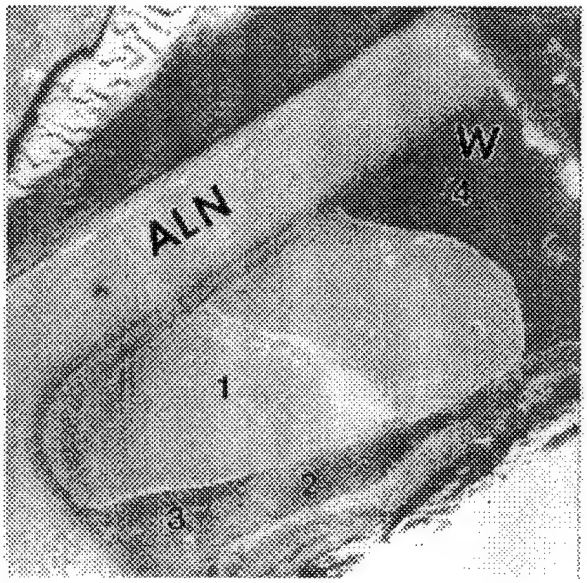

Figure 22. W-Si film surface after reaction with Ni film at 900°C for 1 hour.

4) Pd-W system

A thin palladium and foil (25 microns thick) was placed on top of crystalline W-Si film on AlN substrate, heat treated at 900°C for one hour in argon gas atmosphere. It was found that Pd foil reacts strongly with W-Si film on AlN substrate, as shown in Figure 23. An advancing reaction front on W-Si film surface is clearly seen from the Figure 23. Electron microprobe analysis taken from various regions numbered 1 through 5 showed that concentration of the Pd metal gradually increases, going from location 1 to location 5. Location 1 was initially not in contact with Pd foil during heat treatment, while location 5 was the original position of the Pd foil. Thus, it appears that Pd metal can diffuse ahead of its original position by reacting with W-Si film on AlN surface. Therefore, we conclude that Pd metal can not be used as a pad material on W-Si thin metallization.

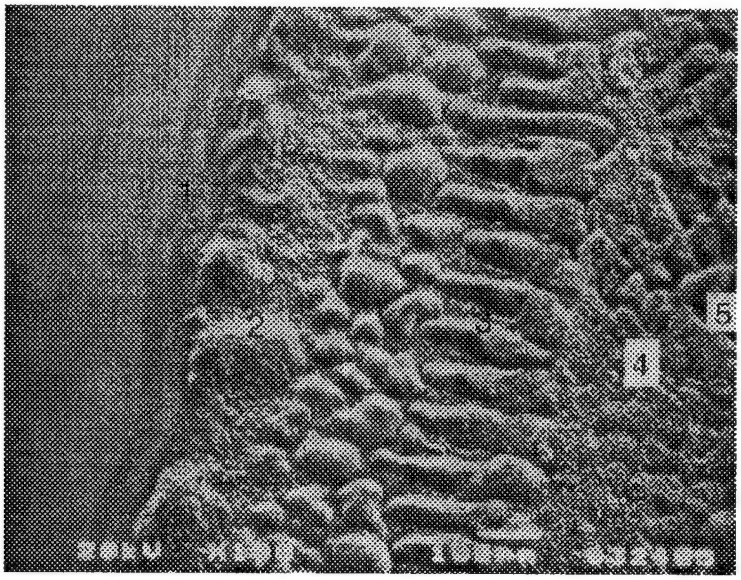

Figure 23. Reaction surface of W-Si film with Pd foil after heat treatment at 900°C in argon.

5) Pt-W system

Pt-W binary phase diagram is an interesting one (see Figure 15 (c)). Both compounds not only have high melting points, but also have no known intermetallic compounds. A platinum foil (25 microns thick) was placed on top of crystalline W-Si film deposited on AlN substrate. Diffusion couple was heat treated at 950°C for 1 hour in argon gas atmosphere. Pt foil reacted strongly with W-Si film in various locations, however, it did not stick every where on the film surface. Figure 24 shows the Pt foil surface after removal from the W-Si film surface. White regions are the holes left in the Pt foil as result of reaction. The mass that was initially present in these locations transferred onto W-Si film surface, as shown in Figure 25. Electron microprobe analysis taken from the vicinity of these residues left on W-Si films, confirmed that Pt was present on W-Si film after the heat treatment. It is likely that Pt-Si compounds were formed since Pt has a strong affinity towards Si.

W-Si/Pt diffusion experiment mentioned above was repeated, at 700°C for 24 hours in argon gas atmosphere. No similar reaction phenomena was observed at 700°C. Pt foil did not reacted with W-Si film in this case and was easily removed from the W-Si surface. Electron microprobe analysis of the W-Si film surface did not reveal any Pt peak after heat treatment. Therefore, Pt can be used as a pad material on W-Si films up to 700°C.

Figure 24. Optical microscopy image of the Pt foil surface (W-Si side) after heat treatment at 950°C for one hour.

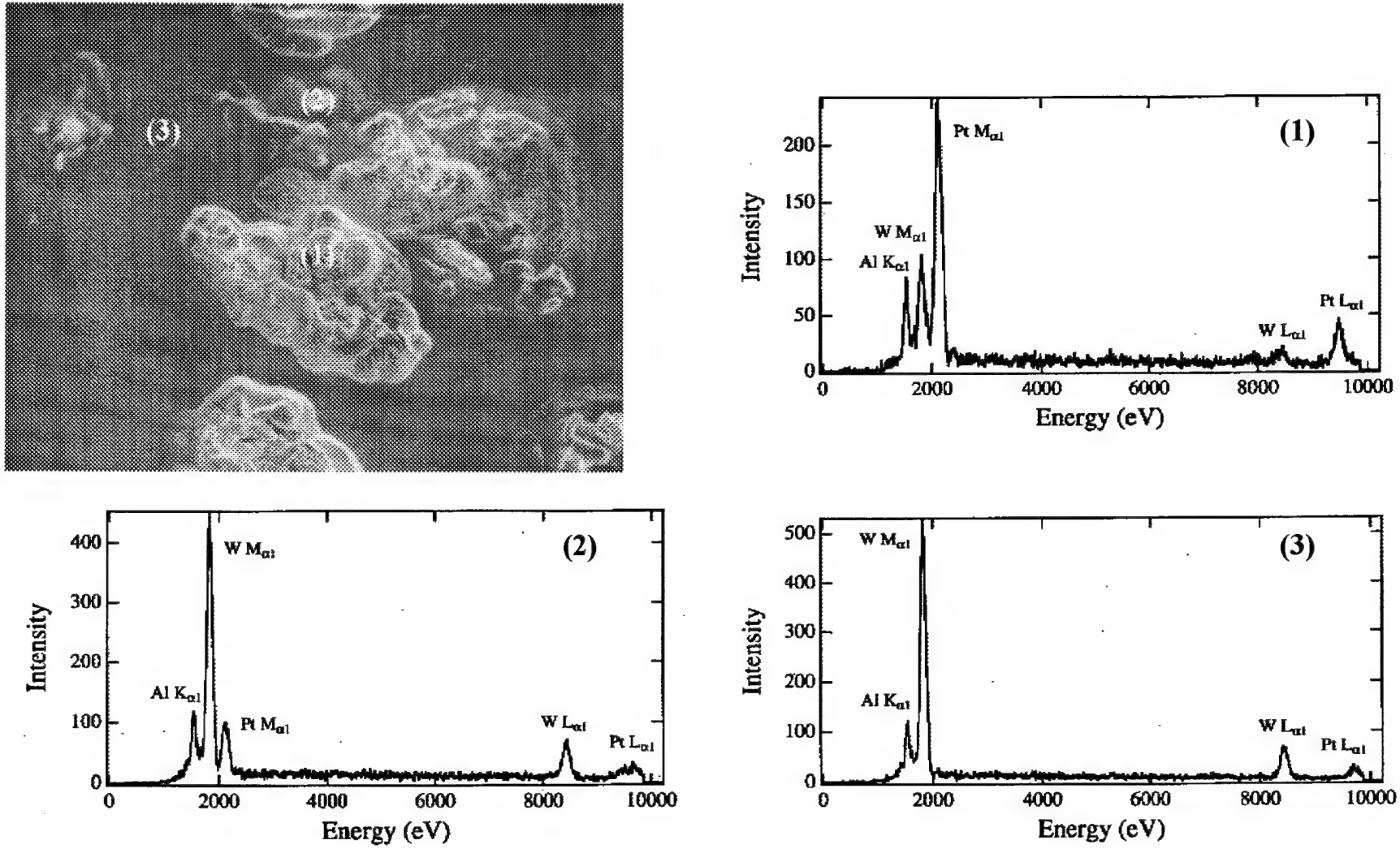

Figure 25. Pt reaction product left on W-Si film surface and EDS spectra from various regions after heat treatment at 950°C.

Compatibility Study between Die Attach Brazes and W-Si Films

For the reasons stated in Task 2, four types of commercially available braze materials were selected for die attach trials. Die attach experiments were performed using n-type SiC single crystal (0.35 mm thick) which had 5x5 mm^2 dimension. Carbon side of the SiC crystal was used without any back-side metallization in all of the brazing trials. A brazing foil of interest with 5x5 mm^2 dimension was placed between the SiC die and the AlN substrate which was metallized with W-Si film developed under Task 1. Whole assembly was placed in a brazing fixture and joined under flowing argon gas. Pull testing was performed after brazing to measure adhesion of die to metallized AlN surface. Electron microprobe analysis was performed on brazing surfaces and polished sample cross-sections to determine the presence of any reaction. Long term compatibility study was performed once the promising die attach material selected. The results are presented below.

1) SiC-Nicoro-WSi-AlN System

Nicoro foil (75 microns thick), which was used as die attach material, contains about 2% nickel in its structure. It is already shown in the previous section that Ni is not compatible with W-Si film. Therefore some reaction was expected to occur in this system during brazing. However, it is estimated that extent of the reaction would be limited because of the small quantity of nickel involved.

Brazing was done in argon gas flow at 1050°C for 30 minutes, using a tungsten mesh heating element. SiC die did not attach well to metallized AlN surface, although it was weakly bonded to the surface after brazing. But, the die was removed easily from the AlN surface without any need for the pull testing. The remaining braze foil was mostly stuck to the die surface, but there was also evidence of extensive reaction on AlN surface, as shown in Figure 26. Significant quantity of Ni, Au and Cu elements were present in W-Si film after brazing trial. This suggests that composition of Nicoro is not compatible with W-Si film developed. Therefore, Nicoro was eliminated as a die attach material with the proposed W-Si metallization films on AlN.

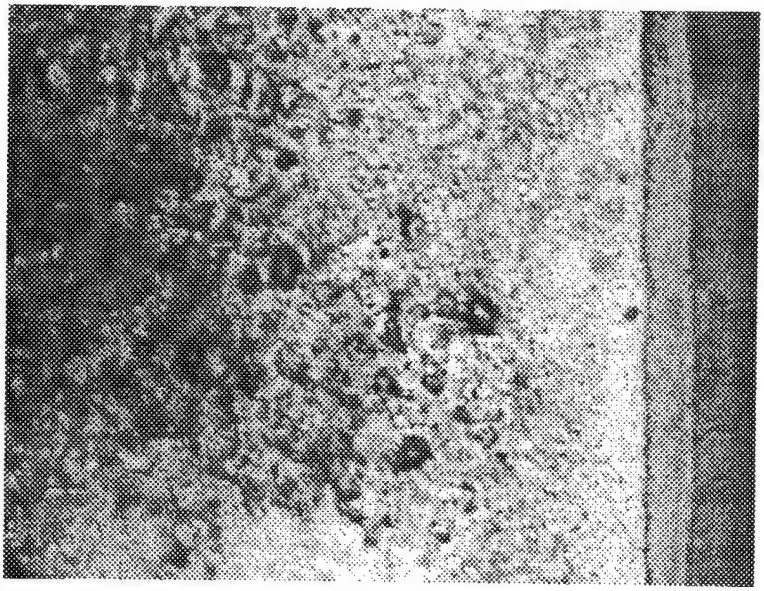

Figure 26. W-Si film surface on AlN after brazing at 1050° using Nicoro foil.

2) SiC- TiCuNi- WSi- AlN System

TiCuNi brazing foil contained more nickel (about 15%) in its structure, therefore, it was expected to be even more reactive than the Nicoro foil used above with W-Si film on AlN. Brazing was done in argon gas atmosphere at 980°C for 20 minutes dwell time, per suggestion of the manufacturer.

TiCuNi brazing foil turned out to be the most active brazing compound considered in this study. Brazing foil reacted with AlN braze fixture and caused W-Si film containing substrate to bond to brazing fixture used. On the other hand, SiC die was easily removed from the brazing surface without any evidence of strong bonding. Examination of the W-Si film surface revealed the presence of strong reaction ahead of the original position of the brazing foil. Figure 27 shows the W-Si film surface containing the brazing compound. The original edge of the brazing foil is between locations marked as 3 and 4 in the Figure 27. Electron microprobe analysis was performed on the locations marked in the Figure 27 and W/Ti, W/Cu, W/Ni, Ti/Cu elemental ratios were calculated from the peak intensity in EDS spectra. Ti/Cu elemental ratio represents the composition variation occurred in the brazing foil, while the other ratios represent the extent of reaction across the sample surface. Ti/Cu elemental ratio is 4.7 in the original brazing foil. The results are presented in Table 11. As shown, there are significant quantity of Ti, Cu and Ni elements ahead of original foil edge. This implicates that especially Cu and Ni components of the brazing compound react with W-Si film to proceed beyond the brazing region, as far as the sample edge. Therefore, TiCuNi braze is not suitable for die attach, not only because of the strong reactivity of the braze with W-Si film, but also lack of wetting on SiC die surface.

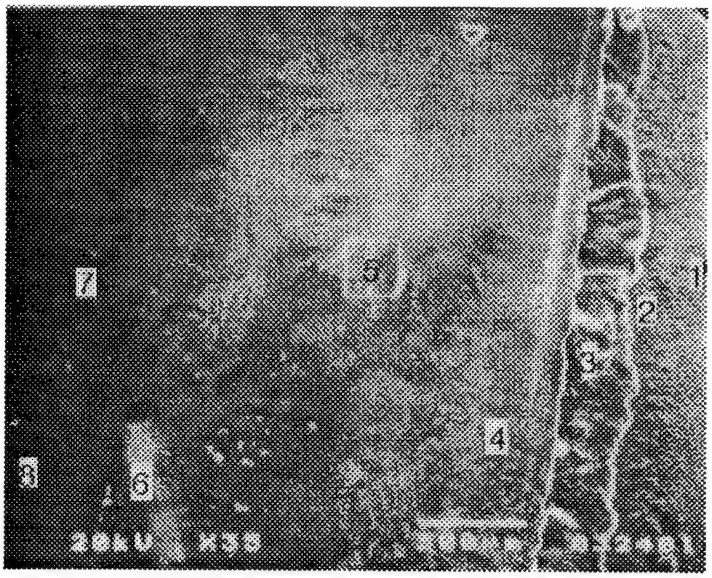

Figure 27. Appearance of W-Si film surface after die attach trial at 980°C using TiCuNi alloy.

3) SiC- Gemco- WSi- AlN System

This brazing alloy is mostly contains Cu and Ge with 0.25 % Ni (see Table 12). Since the nickel amount is very minimal, it was not expected to react with W-Si films on AlN substrate. Brazing was done at 980°C for 30 minutes in argon gas atmosphere.

A strong reaction occurred between the W-Si film and braze used, as shown in Figure 28. Not only SiC die did not attach to brazing compound, but also W-Si film is largely consumed during the brazing at high temperature. This brazing compound is not suitable for die attach applications.

Table 11. Composition change across the brazed region on W-Si Metallized AIN substrate.

Region	Atomic Ratio in Different Regions			
	W/Ti	W/Cu	W/Ni	Ti/Cu
1	0.075	0.69	0.75	9.2
2	0.04	0.62	0.33	13.7
3	0.06	1.0	0.35	16.2
4	0.18	---	---	---
5	0.24	---	---	---
6	0.32	---	---	---
7	0.25	---	---	---

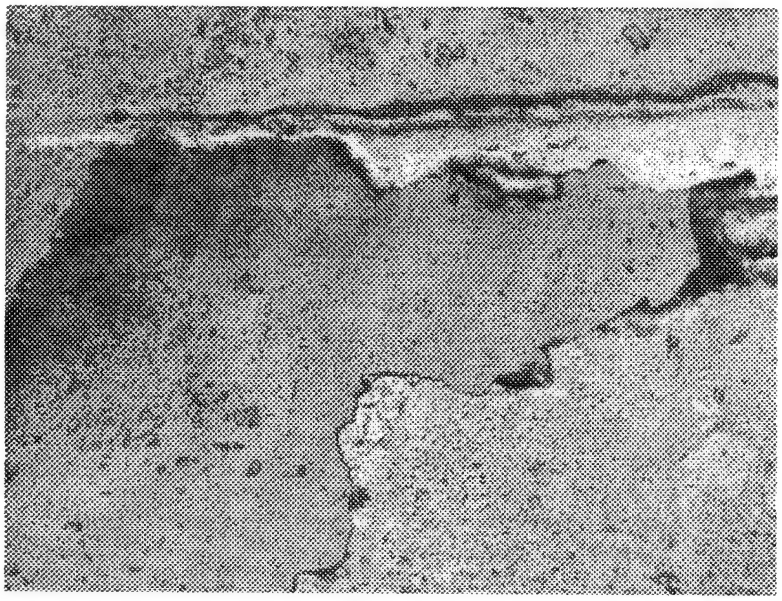

Figure 28. Surface of the W-Si film on AIN substrate after brazing attempt using Gemco braze.

4) SiC- CopperABA-WSi-AIN System

Copper alloy used in these experiments contained up to 2.25% Ti, therefore, the presence of some reaction was anticipated between W-Si film and brazing alloy. Brazing was performed at 1035°C in argon gas atmosphere for 20 minutes. Pull testing of the die attached SiC was performed to measure adhesion to AIN substrate. The results are presented below.

Copper alloy was used successfully to attach the SiC die to W-Si metallized AlN surface. After brazing it was determined that SiC die attached to W-Si metallized AlN surface very strongly. Pull strength of the dies was measured for the two separate experiments. In each case, the failure occurred through the SiC die rather than any of the joining interface with pull strength higher than 2 ksi. The sample was sliced through its thickness and polished to examine braze/SiC and braze/W-Si/AlN interfaces. Figure 29, shows the polished sample cross-section right after brazing. Electron microprobe analysis was performed across the interface along with x-ray dot mapping. The results are shown in Figure 29. It is clear from the Figure 29 that there is no degradation at the W-Copper interface, while some degradation observed at the die/copper interface. This indicates that back side metallization of SiC die may be required, possibly using a similar W-Si film composition so that a reaction barrier can be formed on SiC surface. As shown by Ti x-ray mapping, Ti component of the braze accumulated along the W/AlN and SiC/Braze interfaces. Ti concentration appears to be higher on SiC side of the joint, in addition to copper also penetrating into the SiC die.

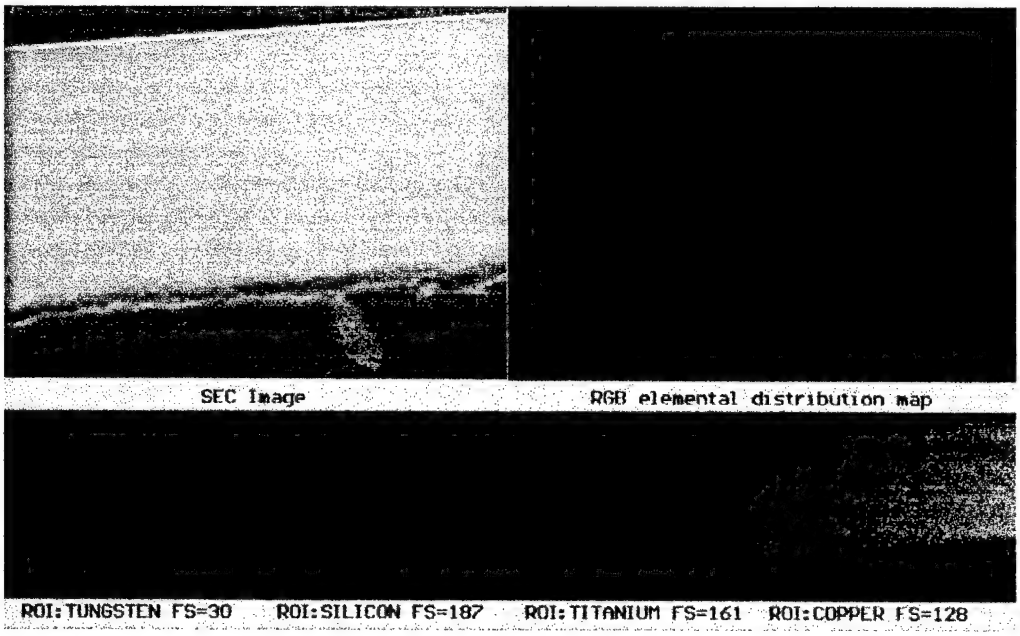

Figure 29. Cross-sectional view and X-ray mapping of SiC die attached to W-Si Metallized AlN surface.

The effect of long term heat treatment on interface stability was investigated after heat treatment of the already die attached sample at 700°C for 22 hours in argon gas atmosphere. As shown in Figure 30, there is no change in W-Si/ copper interface in terms of its stability, however, there is some change at SiC/copper interface. The reaction zone become slightly wider with long term heat treatment. This also indicates that back-side metallization of SiC die is necessary to eliminate the reaction at SiC/copper interface. Copper active metal brazing used, thus, appears to be a feasible candidate as die attach material, provided that a diffusion barrier is applied on SiC back side.

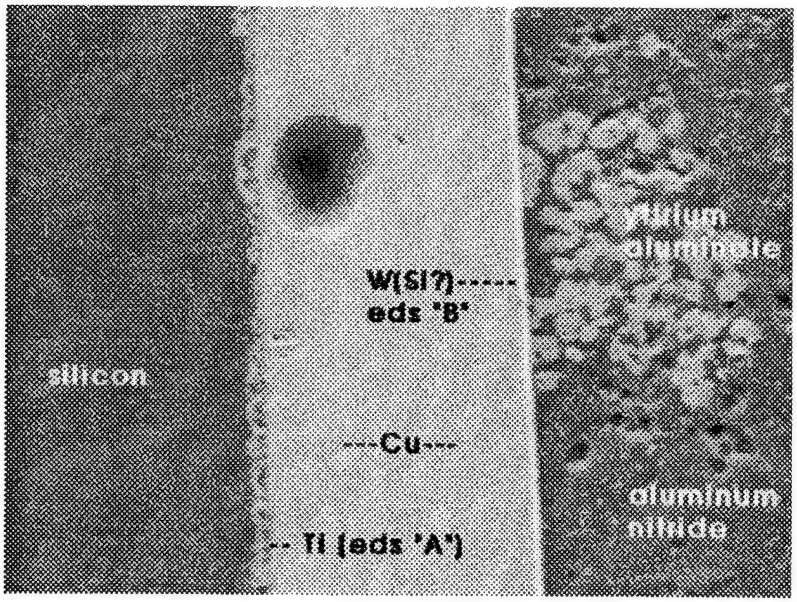

Figure 30. Cross-sectional image of SiC die/copper alloy/W-Si metallized AlN interface after heat treatment 22 hours in argon gas at 700°C.

Compatibility Studies between Wire Materials and Pad Materials Selected

Gold and platinum appear to be the only candidate pad materials suitable for use at 600°C and above when coupled with W-Si metallization layer proposed in this study. Copper has a potential to be employed as a pad material up to 400°C. Compatibility of the pad materials is important with the wires to provide a conductive path between the die and outside world. Therefore, compatibility studies were carried out between Au and Pt pad materials and candidate wire materials selected. In selection of wire materials, high melting point metals were considered because of high temperature operating of the die. Wires should have a high creep resistance since they form a bridge between the die and outside connection terminal. Therefore, Ni, Pd, and Pt metals were selected as potential candidates to investigate their long term high temperature stability against gold and platinum pad materials. In compatibility experiments, foil forms of both metals were sandwiched together and heat treated at 700°C for 8 hours in argon gas atmosphere. Sample cross-sections later were mounted and polished for electron microprobe analysis across the metal/metal interface. No study was performed for the same type of pad and wire material combination (i.e. Pt/Pt or Au/Au), since they are expected to be chemically and thermomechanically compatible. Only the self diffusion of metal could occur in such condition, affecting creep behavior.

Au-Ni System

Gold and nickel show a complete solid-solubility, based on the binary phase diagram shown in Figure 31. Therefore, composition of nickel wire and gold pad is expected to shift towards the equilibrium composition, depending on the quantity of mass available for the reaction. Indeed, after heat treatment of 8 hours at 700°C, significant reaction observed at the Au/Ni interface, as shown in Figure 32. As seen from the figure, electron microprobe analysis taken across the interface shows a series of composition with changing gold/nickel ratio. This means that a single equilibrium composition has not been reached under the conditions of heat treatment used. Such a reactive composition can present a problem to provide a reliable electrical connection between die and pad surface. Therefore, nickel wires do not appear to be a feasible choice of wire material which can be used with Au pad in high temperature (600°C-700°C) packaging applications.

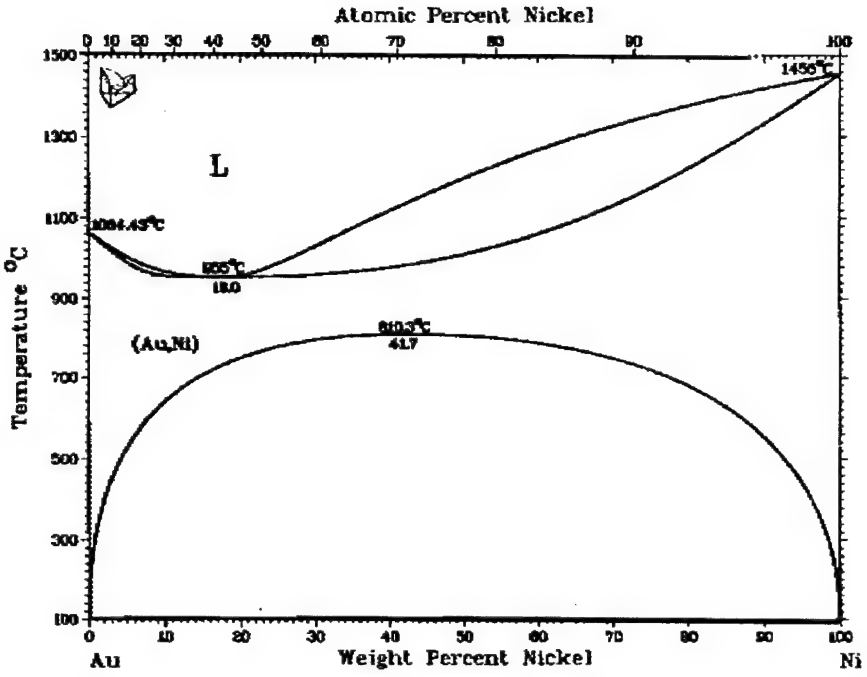

Figure 31. Gold-Nickel Binary Phase Diagram (Massalski, 1986).

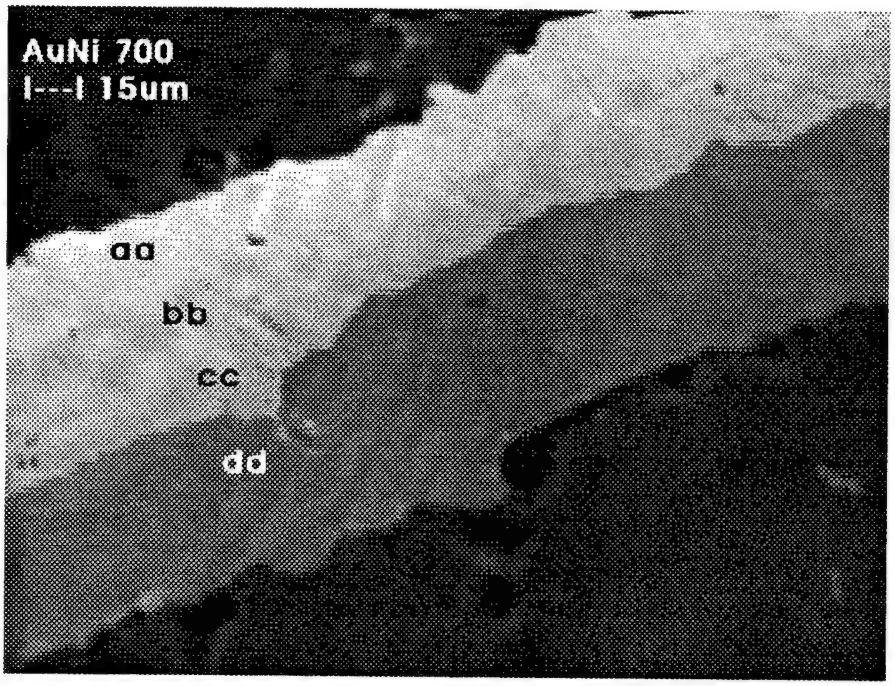

Figure 32. Gold-Nickel interface and EDS spectra after heat treatment at 700°C for 8 hours.

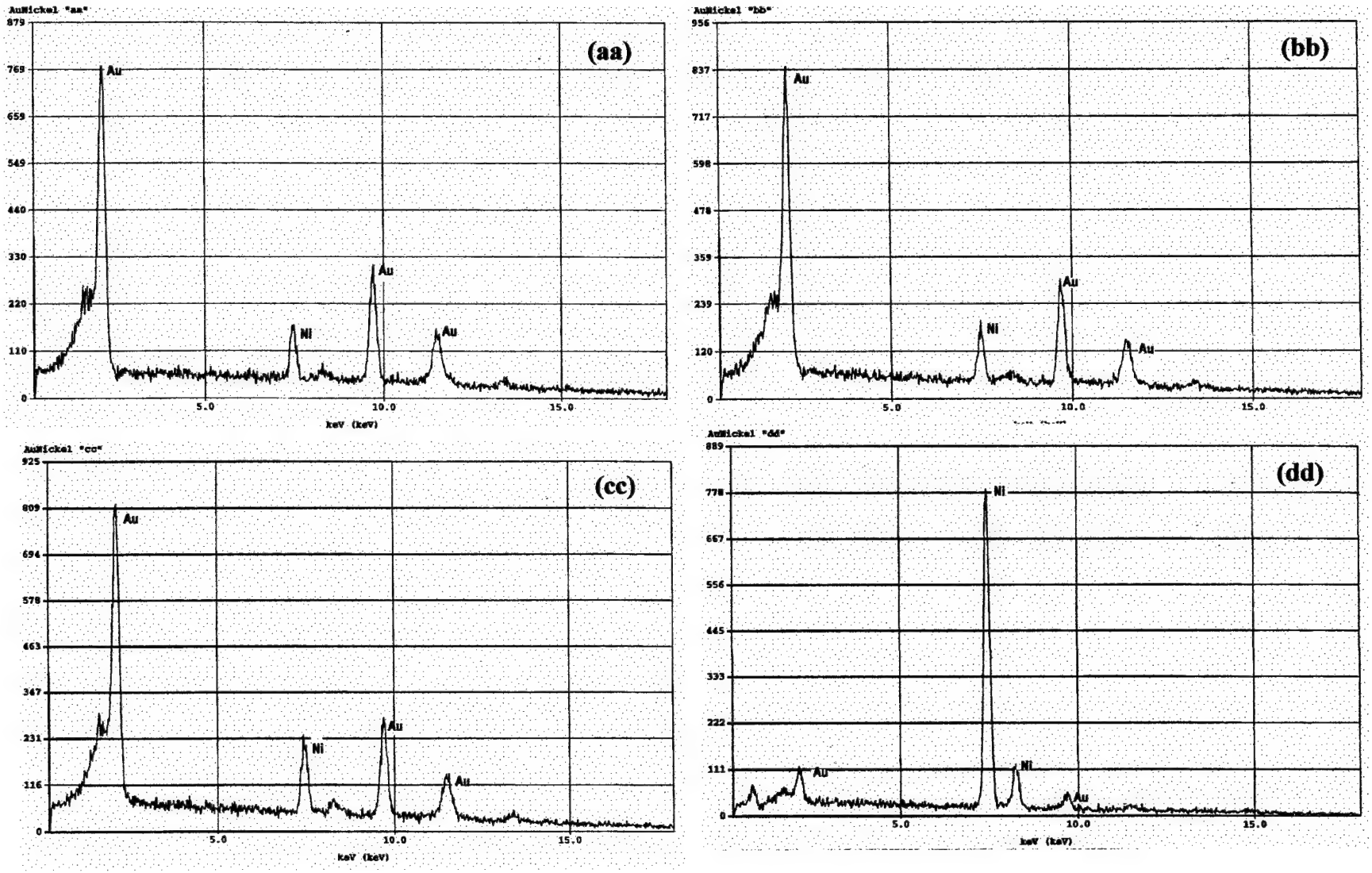

Figure 32. (Continued) Gold-Nickel interface and EDS spectra after heat treatment at 700°C for 8 hours.

Au-Pd System

Au-Pd binary phase diagram is an interesting one and is shown in Figure 33. As seen, Au and Pd form a complete solid solution, but in contrary to the Au-Ni system mentioned above, alloy solidus temperatures are much higher than the melting temperature of gold. In Au-Ni system solidus temperature drops as low as 950°C with alloy formation. Therefore, alloying can occur rather rapidly at die operating temperature of 600°C and above, as shown above. On the other hand, minimum solidus temperature in Au-Pd system is limited with the melting point of pure gold. Therefore, this system appears to be suitable for high temperature applications without any extensive reaction between each element.

One of the polished cross-section of the Au-Pd diffusion couple experiments is shown in Figure 34. The sample was heat treated 8 hours at 700°C. X-ray elemental mapping was performed across the Au/Pd interface and the results are presented in Figure 34. It is clear that, gold and Pd are compatible with each other under the experimental conditions used. Although binary phase diagram suggests the formation of AuPd intermetallic compounds, we did not observe any intermetallic reaction product in our analysis. Furthermore, intermetallic formation in Au-Pd system appears to be speculative, because dotted lines were used in phase diagram. Therefore, based on the our experimental results and known phase relationship in Au-Pd system, it is safe to state that Pd wire can be used in junction with Au pad material without any extensive reaction at the interface up to 700°C.

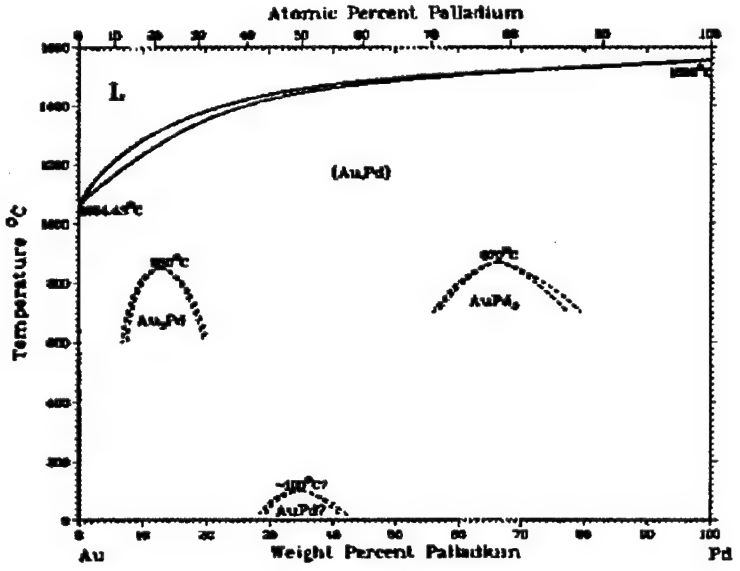

Figure 33. Au-Pd Binary Phase Diagram (Massalski, 1986).

Ni-Pt and Au-Pt Systems

Binary phase diagrams of Au-Pt and Ni-Pt systems are shown in Figures 35 and 36, respectively. It appear from these phase diagrams that if Pt is used as pad material, nickel is not a good wire candidate for high temperature packaging applications since NiPt intermetallic formation. Therefore, nickel is not a choice of wire material. On the other hand, Au wire is a possible candidate to be used with Pt pad, because the binary system not only shows an increasing solidus temperature with alloying, but also do not present any stable intermetallic formation.

In summary, Pd and Pt wires could be used with Au pads, while Au wire can be used with Pt pad in designing of package for high temperature applications.

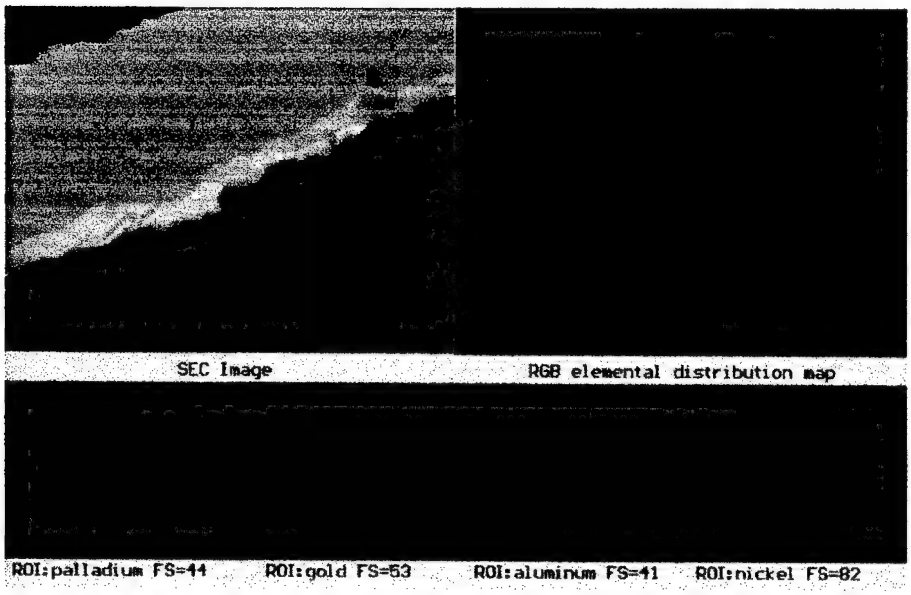

Figure 34. Gold-Palladium interface after heat treatment at 700°C for 8 hours.

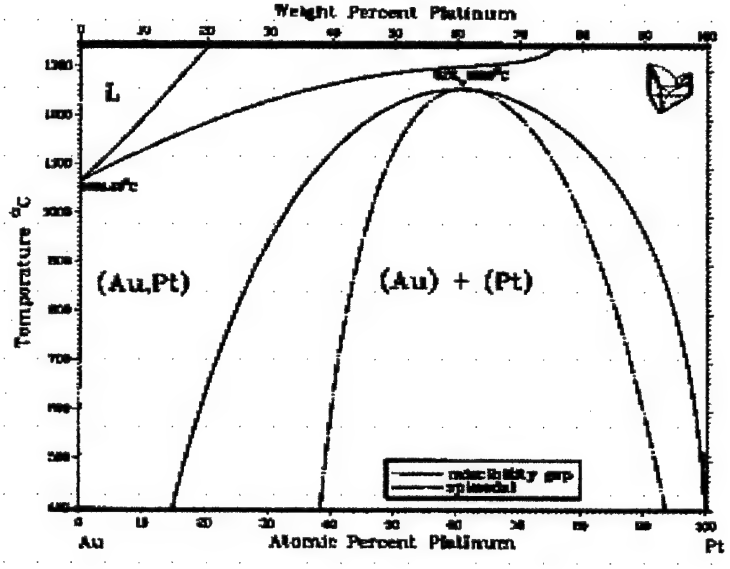

Figure 35. Au-Pt binary phase diagram (Massalski, 1986).

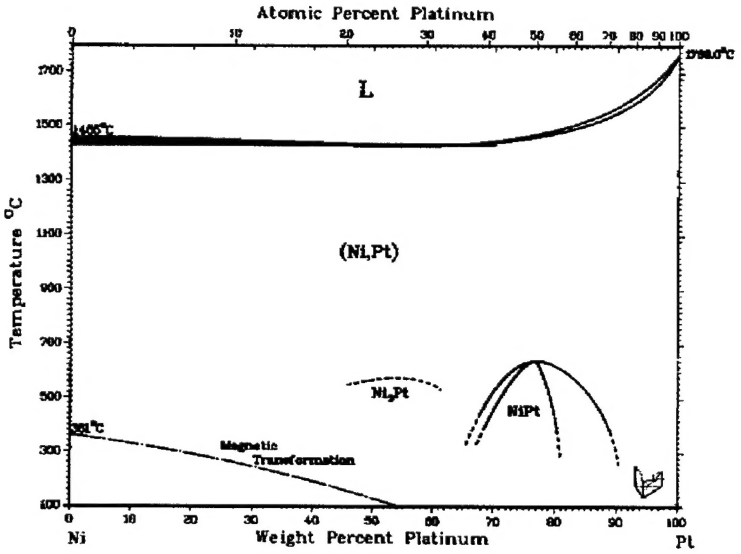

Figure 36. Ni-Pt binary phase diagram (Massalski, 1986).

Refractory Mo-Mn Thick Film for AlN Metallization and its Compatibility with Pt

During the course of this project thick film metallization of the AlN was also studied for high temperature packaging applications. A commercially available Mo-Mn thick film paste was modified to improve the adhesion to AlN substrate. A serpentine pattern was screen printed on lapped AlN substrates. Samples were heat treated at 1200°C for 30 minutes in H_2/N_2 gas mixture. Some of the samples were electroplated with nickel after heat treatment. Sheet resistance and pull strengths were determined after various heat treatment conditions: a) as-fired, b) after 24 hours heat treatment at 700°C in argon atmosphere, c) after thermal cycling tests to 1100°C for 10 times in argon atmosphere, and d) after heat treatment at 1100°C in argon atmosphere 30 minutes. The results are shown in Table 12.

Table 12. Sheet resistance and pull strength of the modified Mo-Mn thick film paste on AlN substrates.

Mo-Mn Thick Film				
	As-fired	24 hrs at 700°C	10x thermal cycle	0.5 hrs 1100°C
Sheet Resistance (ohms/□)	0.0256	0.0264	0.0204	0.021
Average Pull Strength (ksi)	11.6	12.7	13.1	11.7
Range (ksi)	9.3-13.2	12.3-13.2	12.4-13.7	11.0-12.0
Ni Plated Mo-Mn Thick Film				
Sheet Resistance (ohms/□)	0.0254	0.0575	-----	0.265
Average Pull Strength (ksi)	8.7	10.9	-----	7.6
Range (ksi)	7.4-10.1	8.9-12.2	---	7.0-8.3

As seen in Table 12, the average pull strength of the Mo-Mn thick film samples were greater than 10 ksi for every heat treatment condition employed. Pull strength and sheet resistance of the thick films did not appear to decrease with heat treatment up to 1100°C. This is a very significant result since currently no reliable refractory thick film metallization available for AlN substrates. However, sheet resistance of the nickel plated samples shows an order of magnitude increase after heat treatment 30 minutes at 1100°C, while pull strength drops below 10 ksi range. Degradation of the thick film properties could be due to the reactions between Ni and Mo metals at high temperature. Mo is a refractory metal and shows a very similar behavior to tungsten. Since it was already shown in the previous sections that W and Ni react very strongly, there may be a similar reaction taking place between Mo and Ni. Thus, Mo-Mn thick film should be investigated further to establish its suitability for high temperature use.

We examined the short and long term compatibility of Mo-Mn thick film metallized AlN substrates with Pt at 950°C and 700°C, respectively. No nickel plating was used in these thick film samples. A platinum foil (25 microns thick) was coupled with Mo-Mn thick film formed at 1200°C. Diffusion couple samples were heat treated one hour at 950°C and 24 hours at 700°C. Pt foil does not attach to Mo surface after each heat treatment, suggesting no reaction occurs between Pt foil and Mo surface.

6. PHASE II CONCLUSIONS

The following conclusions can be drawn from the Phase II study:

- W-Si film composition can be modified using co-sputtering method to yield either a single phase or a mixture of W, WSi_2, and W_5Si_3 phases by changing the Si/W ratio.
- When the Si/W ratio of the as-sputtered film is less than 0.7, the film composes of more than 90% tungsten and 10% W_5Si_3 upon heat treatment.
- When the Si/W ratio is higher than 1.5, the resulting film is single WSi_2 phase.
- W-Si metallization with Si/W ratio is less than 0.7, can be used reliably on AlN at temperatures higher than 600°C for high temperature packaging applications.
- Pure tungsten film does not adhere to AlN, however, the presence of Si improves the adhesion of W to AlN substrates without significant increase in the sheet resistivity.
- While all the films present a good film integrity on AlN surface in as-deposited condition, crystallization process after heat treatment introduces macro defects in the film structure for all the composition with Si/W ratio is higher than 0.7, therefore, limited the number of compositions that can be considered for thin film applications.
- Si doped W thin films were found to be an excellent choice for metallization of AlN substrates for high temperature use. Neither pull strength, nor sheet resistance of the W-Si films degrade after short, long term heat treatments up to 1300°C and thermal cycle conditions up to 1100 C. While the pull strengths higher than 10 ksi were maintained, sheet resistance was less than 1 ohms/□ after heat treatment 65 hours at 1300°C.
- Cross-sectional TEM analysis on heat treated samples also showed that W-Si films strongly attached to AlN surface, while pure tungsten did not adhere to AlN surface.
- Adhesion of W to AlN surface appears to be due to the diffusion of Si from the W film into the AlN surface, creating a strong transition interface.
- Literature review was made to select wire, die attach, and pad materials compatible with the W-Si alloy developed.

- Among the various pad materials studied (Cu, Ni, Au, Pt, and Pd) only Au and Pt found to be stable pad material with W-Si film after heat treatment as high as 700°C. While Ni and Pd strongly reacted with W-Si films, Cu showed some limited reaction at 700°C, but no reaction at 400°C. Therefore, Au and Pt are the choice of materials for pad applications to be used with W-Si films developed on AlN packages. Copper could also be considered for temperatures up to 400°C.
- Monometallic Au-Au, Pt-Pt, Cu-Cu, Pd-Pd, and Au-Pt couples can be used as bond pad and bond wire above 600°C. However, only Au and Pt were found to be compatible with W-Si metallization on AlN, therefore, if W-Si is selected as the substrate metallization Au-Au and Pt-Pt interconnections should be used. Pd-Au, Cu-Au, and Au-Ni can be used at temperatures up to 400°C, however, their long term reliability should be established.
- Among the various die attach materials considered, only copper active brazing compound found to be stable against the W-Si film, even after 22 hours at 700°C. Nickel and germanium based die attach brazes were most reactive with W-Si films developed.
- Limited reaction between the SiC die and copper braze alloy occurred; however, a SiC back-side metallization should eliminate this problem. Therefore, copper brazing alloy appears to be a good candidate for SiC die attach.
- Traditional Mo-Mn thick film pastes can be modified to obtain adherent thick films on AlN substrates. Thick film Mo is also suitable for high temperature packaging applications up to 1000°C without significant compromise in pull strength and sheet resistance of the film.
- Plated nickel is not compatible with Mo thick film, while Pt can be used safely with Mo thick films up to 700°C without any evidence of reaction.

In summary, a new metallization scheme is proposed for the packages operating at 600°C and beyond. Substrate is made of AlN metallized with W-Si thin film containing less than 10% W_5Si_3 in its structure. Interconnections should be active copper brazing for die attach up to 700°C, Au or Pt bond pad and Au and Pt wires for up to 700°C.

7. REFERENCES

ASM International Metals Handbook: Metallography, Structures and Phase Diagrams (1973) Vol. 8, 8th Edition, ASM International, Metals Park, OH.

Blum, J. (1989) Aluminum Nitride Data Sheet, Toshiba Corporation.

Gehman, B. (1980) "Bonding Wire Microelectronic Connections," *IEEE Trans. CHMT*, Vol. CHMT-3, p. 375.

Hall, P.M., and Morabito, J.M. (1978) "Diffusion Problems in Microelectronic Packaging," *Thin Solid Films*, Vol. 53, p. 175.

Konsowski, S. G. (1993) "Advanced Electronic Packaging Materials, and Processes," in *Electronic Materials and Processes Handbook*, Ed. C. A., Haper and R.M. Sampson, Chapt. 11, McGraw-Hill, New York, NY.

Mahefkey, T. (1994) "Thermal Management of High Temperature Power Electronics - Limitations and Technology Issues," *Trans. Second Int. High Temp. Elect. Conf.*, p. IX-21.

Massalski, T.B. (1986) "Binary Allow Phase Diagrams," Vol. I and II, ASM International, Metals Park, OH.

Tummala, R. R., and Rymaszewski, E. J. (1989) *Microelectronics Packaging Handbook*, VNR, NY.

Waite, G. C., (1981) "The Automotive Environment - Its Impact on Electronic Design," *ISHM Proc.*, p. 226.

Werdecker, W., and Aldinger, F. (1984) "Aluminum Nitride: An Alternative Ceramic Substrate for High Power Applications in Microcircuits," *IEEE Trans. CHMT*, Vol. 7, p. 399.

Yang, H., Turlik, J. and Murty, K L. (1993) "The Evaluation of Mechanical Behavior of Die Attach Materials for Electronic Packaging Application," *Proc. 8th Elect. Matl. Proces. Cong.*, p. 55, ASM International, Metals Park, OH.